A multi-scale model for the planetary and synoptic motions in the atmosphere

S. I. Dolaptchiev *

Institut für Atmosphäre und Umwelt, Goethe-Universität Frankfurt, Frankfurt am Main, Germany

R. Klein

FB Mathematik & Informatik, Freie Universität Berlin, Berlin, Germany

* *Corresponding author address:* S. I. Dolapthciev, Institut für Atmosphäre und Umwelt, Goethe-Universität Frankfurt, Altenhöferallee 1, 60438 Frankfurt (Main), Germany

E-mail: Dolaptchiev@iau.uni-frankfurt.de

ABSTRACT

A reduced asymptotic model valid for the planetary and synoptic scales in the atmosphere is presented. The model is derived by applying a systematic multiple scales asymptotic method to the full compressible flow equations in spherical geometry. The synoptic scale dynamics in the model is governed by modified quasi-geostrophic equations which take into account planetary scale variations of the background stratification and of the Coriolis parameter. The planetary scale background is described by the planetary geostrophic equations and a new closure condition in the form of a two-scale evolution equation for the barotropic component of the background flow. This closure equation provides a model revealing an interaction mechanism from the synoptic scale to the planetary scale.

To obtain a quantitative assessment of the validity of the asymptotics, the balances on the planetary and synoptic scales are studied by utilizing a primitive equations model. For that purpose spatial and temporal variations of different terms in the vorticity equation are analyzed. It is found that for planetary scale modes the horizontal fluxes of relative and planetary vorticity are nearly divergence free. It is shown that the results are consistent with the asymptotic model.

1. Introduction

Many atmospheric phenomena important for the low-frequency variability (periods longer than 10 days) are characterized by planetary spatial scales, i.e., scales of the order of the earth's radius $\approx 6 \times 10^3$ km. Such phenomena are the orographically and thermally induced quasi-stationary Rossby waves, eddy-driven teleconnection patterns such as the Northern and Southern Annular Modes (NAM,SAM), Pacific/North American Pattern (PNA) or the North Atlantic Oscillation (NAO), large-scale ultralong persistent blockings and the polar/subtropical jet. On the other hand the synoptic eddies, which are responsible for the variability with periods of 2-6 days, have as a characteristic length scale the internal Rossby deformation radius (Pedlosky 1987), which is around 1000 km. Although the spatial and temporal separation between the planetary and synoptic scale atmospheric motion is not so pronounces as in the ocean, the different scales are evident in spectral analyses of tropospheric data: observations (e.g. Blackmon 1976; Fraedrich and Böttger 1978; Fraedrich and Kietzig 1983) as well as simulations (e.g. Gall 1976; Hayashi and Golder 1977) show the presence of isolated peaks in the wavenumber-frequency domain. Fig. 1 (taken from Fraedrich and Böttger (1978)) displays three such peaks in the spectrum of the meridional geostrophic wind. There is a maximum associated with the quasi-stationary Rossby waves with zonal wavenumber $k =$ 1-4 and with periods larger than 20 days. The other two maxima at $k =$ 5-6 and at $k =$ 7-8 result from the synoptic waves. These are eastward propagating long and short waves associated with different background stratifications (Fraedrich and Böttger 1978). The overall picture of three maxima persists during the different seasons for the Northern Hemisphere, indicating a separation between the planetary and the synoptic scales. However, the interactions between the two scales are of great relevance to the atmospheric dynamics as stressed in many studies (e.g. Hoskins et al. 1983).

The fast growth of computational resources in atmospheric sciences over the last decades leads to a huge increase of complexity in atmospheric models. This becomes apparent, if one considers the development of the comprehensive general circulation models (GCMs). However, as simulations with those models become more and more closer to observations, the interpretation of the results with regard to improving the models as well as the understanding of the climate system becomes more difficult. This stresses the importance of simplified models, utiliezed for studies of many aspects of the circulation, such as instability, wave propagation and interaction. As discussed by Held (2005), the development of a hierarchy of reduced models provides a tool for systemetic improvement of the comprehensive models and thereby contributes to our understanding of the climate system .

One prominent example (if not the most prominent) of simplified model equations is the quasi-geostrophic (QG) theory (Charney 1948), which describes the baroclinic generation and evolution of the synoptic scale eddies. This theory is derived under the assumption of a horizontally uniform background stratification and small variations of the Coriolis parameter (Pedlosky 1987), an assumption which is often violated if one considers motions on a planetary scale (such as the one mentioned in the first paragraph). Reduced model equations, which do not make use of the latter assumption and model planetary scale motions, are the planetary geostrophic equations (PGEs; Robinson and Stommel 1959; Welander 1959; Phillips 1963). The PGEs describe balanced dynamics, however the relative vorticity advection is absent in the potential vorticity (PV) equation (the consequences we will discuss later on). Much effort has been made to develop simplified models valid for the planetary and synoptic scale and for the interactions between the two scales. Pedlosky (1984) proposed a two-scale model for the ocean circulation, where the dynamics on the large scale is governed by the PGEs and the dynamics on the small scale by a modified QG equation, which is influenced by the large scale. Mak (1991) incorporated in the QG model effects due to spherical geometry of the earth by considering higher order terms. Vallis (1996) introduced the geostrophic PV model, which can be reduced to QG or to PG model by imposing an appropriate scaling. Numerical simulations (Mundt et al. 1997) with the geostrophic PV model showed, that this model improves the circulation patterns over the latter classical models. Luo developed multi-scale models for planetary-synoptic interaction and applied them for studies of blockings (Luo et al. 2001; Luo 2005) and NAO dynamics (Luo et al. 2007).

In a previous paper (Dolaptchiev and Klein 2009, hereafter DK) we presented reduced model equations valid for one particular regime of planetary scale atmospheric motions, we refer to this regime as the planetary regime (PR). In the PR we consider the planetary horizontal scales and a corresponding advective time scale of 7 days (see Fig. 2). The PR model includes the PGEs and a novel evolution equation for the barotropic flow. As discussed in DK, in applications to the atmosphere of the PGEs the barotropic flow has to be specified, because there is no advection of relative vorticity in the PGEs. The novel evolution equation in the PR provides a prognostic alternative relative to temperature-based diagnostic closures for the barotropic flow adopted in reduced-complexity planetary models (Petoukhov et al. 2000). The PR model takes into account large variations of the background stratification and of the Coriolis parameter, but it does not describe the synoptic eddies. This limitation motivate an extension of the validity region of the single-scale PR-model to the synoptic spatial and temporal scales (see Fig. 2). In this paper we apply the same asymptotic approach from DK, but utilizing now a two scale expansion resolving both the planetary and the synoptic scales. In doing so we can take into account in a systematic manner the interactions between the planetary and the synoptic scales with particular attention payed on the barotropic component of the background flow. Part of the derived model equations can be regarded as the anelastic analogon of Pedlosky's two scale model for the large-scale ocean circulation (Pedlosky 1984). But whereas the latter model describes only interaction from the planetary to the synoptic scale, in the present model there is an additional planetary scale evolution equation for the vertically averaged pressure which provides a reverse interaction (from the synoptic to the planetary scale dynamics) in the form of momentum fluxes due to the synoptic scale velocity field. This type of feedback on the planetary scale differs from the one recently proposed by Grooms et al. (2011), where the PGEs are influenced by the synoptic scale through eddy buoyancy fluxes. We have to point out, that momentum fluxes due to synoptic eddies are commonly considered as an interaction mechanism acting on atmospheric planetary scale barotropic flow (e.g., Luo (2005); Luo et al. (2007)), however to our knowledge not in the context of PGEs.

The outline of this paper is as follows: in section 2 we briefly discuss the asymptotic method applied for the derivation of the two scale model. Key steps in the derivation are presented in section 3. The asymptotic model equations are summarized and discussed in section 4. We compare the results from the asymptotic analysis with numerical simulations with a primitive equations model in section 5. A concluding discussion can be found in section 6.

2. Asymptotic approach for the derivation of reduced models for the planetary and synoptic scales

a. Asymptotic representation of the governing equations

We utilize the multiple scales asymptotic method of Klein (2000, 2004, 2008). It has been applied in the development of reduced models, e.g., for the tropical dynamics (Majda and Klein 2003), deep mesoscale convection (Klein and Majda 2006), moist boundary layer dynamics (Owinoh et al. 2011) and concentrated atmospheric vortices (Päschke et al. 2012).

Here we give a brief summary of the treatment of the governing equations for a compressible fluid with spherical geometry in the asymptotic framework (for the complete discussion we refer to DK). First, we nondimensionalize the equations by using as reference quantities: the thermodynamic pressure $p_{ref} = 10^5\,\mathrm{kg\ m^{-1}\,s^{-2}}$, the air density $\rho_{ref} = 1.25\,\mathrm{kg\,m^{-3}}$ and a characteristic flow velocity $u_{ref} = 10\,\mathrm{m\,s^{-1}}$. The above quantities define further the scale height $h_{sc} = p_{ref}/g/\rho_{ref} \approx 10\,\mathrm{km}$ ($g = 9.81\,\mathrm{m\,s^{-2}}$ is the gravity acceleration) and its time scale $t_{ref} = h_{sc}/u_{ref} \approx 20\,\mathrm{min}$. We introduce a small parameter ε as the cubic root of atmosphere's global aspect ratio

$$\varepsilon = \left(\frac{a^*\Omega^2}{g}\right)^{\frac{1}{3}}, \tag{1}$$

where $a^* \approx 6 \times 10^3\,\mathrm{km}$ is the earth's radius and $\Omega \approx 7 \times 10^{-5}\,\mathrm{s^{-1}}$ the earth's rotation frequency. With these estimates we find $\epsilon \sim 1/8 \ldots 1/6$, and henceforth consider asymptotic limits for $\epsilon \ll 1$. Next, the nondimensional Mach, Froude and Rossby numbers in the governing equations are expressed in terms of ε, which is referred to as a distinguished limit. The coupling of all characteristic numbers in terms of only one small parameter is motivated by the fact, that asymptotic expansions of simple systems (such as the linear damped oscillator) give non-unique results if multiple independent parameters are used. With the present specific coupling a variety of classical models can be rederived, see also Klein (2008) for further discussion of the distinguished limit. An alternative interpretation of ε to the one in (1), is that ε equals the Rossby number for the synoptic scales (see Fig. 2 for the synoptic length scaling). Introducing the distinguished limit, the nondimensional governing equations in spherical coordinates take the form

$$\frac{d}{dt}u - \varepsilon^3\left(\frac{uv\tan\phi}{R} - \frac{uw}{R}\right) + \varepsilon(w\cos\phi - v\sin\phi) = -\frac{\varepsilon^{-1}}{R\rho\cos\phi}\frac{\partial p}{\partial\lambda} + S_u\,, \tag{2}$$

$$\frac{d}{dt}v + \varepsilon^3\left(\frac{u^2\tan\phi}{R} + \frac{vw}{R}\right) + \varepsilon u\sin\phi = -\frac{\varepsilon^{-1}}{R\rho}\frac{\partial p}{\partial\phi} + S_v\,, \tag{3}$$

$$\frac{d}{dt}w - \varepsilon^3\left(\frac{u^2}{R} + \frac{v^2}{R}\right) - \varepsilon u\cos\phi = -\frac{\varepsilon^{-4}}{\rho}\frac{\partial p}{\partial z} - \varepsilon^{-4} + S_w\,, \tag{4}$$

$$\frac{d}{dt}\theta = S_\theta\,, \tag{5}$$

$$\frac{d}{dt}\rho + \frac{\varepsilon^3\rho}{R\cos\phi}\left(\frac{\partial u}{\partial\lambda} + \frac{\partial v cos\phi}{\partial\phi}\right) + \rho\frac{\partial w}{\partial z} + \frac{\varepsilon^3 2w\rho}{R} = 0\,, \tag{6}$$

$$\rho\theta = p^{\frac{1}{\gamma}}\,, \tag{7}$$

where λ, ϕ and z stay for longitude, latitude and altitude. The nondimensional variables p, ρ and θ denote pressure, density and potential temperature; u, v and w are the zonal, meridional and vertical velocity components. $S_{u,v,w}$ and S_θ represent momentum and diabatic source terms,γ is the isentropic exponent and the operator d/dt is given by

$$\frac{d}{dt} = \frac{\partial}{\partial t} + \frac{\varepsilon^3 u}{R\cos\phi}\frac{\partial}{\partial\lambda} + \frac{\varepsilon^3 v}{R}\frac{\partial}{\partial\phi} + w\frac{\partial}{\partial z}\,, \tag{8}$$

where $R = a + \varepsilon^3 z$ (a order one constant). We want to stress that the reference quantities used for the non-dimensionalization, although valid vor a variety of flow regimes, might not be characteristic for the particular regime of interest, e.g., the scale height is not an appropriate horizontal scale for the description of planetary and synoptic scale atmospheric motions. Within the asymptotic approach a particular regime of interest can be studied, if rescaled coordinates together with an asymptotic series expansion of the dependent variables are introduced based on physical arguments and intuition. The scaling and the asymptotic expansion should reflect the relevant physical processes in the flow regime of interest.

b. *Coordinates Scaling for the two scale Planetary Regime*

The coordinates resolving the planetary and synoptic time and spatial scales are summarized in Table 1. The planetary coordinates λ_P and ϕ_P are suitable for the description of horizontal variations of the order of the earth's radius a^*. The corresponding planetary advective time scale is about 7 days and is resolved by t_P. The synoptic scale variables λ_S, ϕ_S and t_S describe motions with characteristic length scales of 1 000 km $\sim \varepsilon a^*$ and with a time scale of about 1 day. For the vertical coordinate z no scaling is required. Since this coordinate was nondimensionalized using the scale height h_{sc}, it describes motions spreading through the full depth of the troposphere. A more detailed discussion of the scaling can be found in DK, the validity range of the two-scale Planetary Regime is sketched in Fig. 2.

We assume that each dependent variable from (2) - (7) can be represented as an asymptotic series in terms of ε

$$U(\lambda, \phi, z, t; \varepsilon) = \sum_{i=0}^{\infty} \varepsilon^i U^{(i)}(\lambda_P, \phi_P, \lambda_S, \phi_S, z, t_P, t_S)\,, \qquad (9)$$

where $U = (u, v, w, \theta, \rho, \pi)$. Note that the time and horizontal spatial coordinates of the individual terms in the series resolve both the planetary and synoptic scales.

c. *Sublinear growth condition*

In order to guarantee a well defined asymptotic expansion (9), we have to require that $U^{(i)}$ grows slower than linearly in any of the synoptic coordinates. This requirement is known as the sublinear growth condition. Suppose, X_S denotes one of the synoptic coordinates λ_S, ϕ_S, t_S and X_P the corresponding planetary coordinate λ_P, ϕ_P or t_P. Since we have $X_S = X_P/\varepsilon$, we can formulate the sublinear growth condition for the coordinate X_S as

$$\lim_{\varepsilon \to 0} \frac{U^{(i)}(\ldots, X_S)}{X_S + 1} = \lim_{\varepsilon \to 0} \frac{U^{(i)}(\ldots, \frac{X_P}{\varepsilon})}{\frac{X_P}{\varepsilon} + 1} = 0\,, \qquad (10)$$

where all coordinates except X_S are held fixed with respect to ε in the limit process. An immediate consequence from the last constraint is the disappearing of averages over X_S of terms, which can be represented as derivatives with respect to X_S. In particular we have

$$\overline{\frac{\partial}{\partial X_S} U^{(i)}}^{X_S} = 0\,. \tag{11}$$

Here the averaging operator $\overline{()}^{X_S}$ is defined as

$$\overline{U^{(i)}}^{X_S}(\ldots) = \lim_{\varepsilon\to 0} \frac{\varepsilon}{2L_S} \int\limits_{\frac{X_P}{\varepsilon}-\frac{L_S}{\varepsilon}}^{\frac{X_P}{\varepsilon}+\frac{L_S}{\varepsilon}} U^{(i)}(\ldots, X_S)\,\mathrm{d}X_S\,, \tag{12}$$

where L_S is some characteristic averaging scale for the coordinate X_S. Eq. (11) implies that in the asymptotic analyses the synoptic scale divergence of a flux has no effect on the planetary scale dynamics, when the synoptic scale averaging (12) is applied. This follows directly from the sublinear growth condition (10) and we will make extensive use of it in the derivation of the reduced model equations.

d. *Assumptions for the background stratification*

As already mentioned the classical QG theory takes into account only small deviations from a constant background distribution of the potential temperature. This background is assumed to be horizontally uniform and is characterized by a Brunt-Väisälä frequency of $\mathcal{O}(10^{-2})$ s^{-1}, which in nondimensional form implies a horizontally uniform $\mathcal{O}(\varepsilon^2)$ background potential temperature (Majda and Klein 2003). Similarly as in DK, we allow here $\mathcal{O}(\varepsilon^2)$ variations on the planetary scales of the background potential temperature distribution. In order to remain consistent with the assumptions in the QG theory we consider an order of magnitude smaller variations on the synoptic spatial and temporal scales, namely $\mathcal{O}(\varepsilon^3)$. Thus the expansion for the potential temperature takes the form

$$\theta = 1 + \varepsilon^2\Theta^{(2)}(\lambda_P, \phi_P, z, t_P) + \varepsilon^3\Theta^{(3)}(\lambda_P, \phi_P, \lambda_S, \phi_S, z, t_P, t_S) + \mathcal{O}(\varepsilon^4)\,. \tag{13}$$

Next, we proceed with the asymptotic derivation of the reduced equations.

3. Derivation of the Planetary Regime with synoptic scale interactions

a. *Asymptotic expansion*

1) *Notation*

From here on we use the following notation

$$\boldsymbol{X}_S = (\lambda_S, \phi_S, t_S), \boldsymbol{X}_P = (\lambda_P, \phi_P, t_P) \tag{14}$$

$$f = \sin\phi_P\,, \beta = \frac{1}{a}\frac{\partial}{\partial\phi_p}\sin\phi_P\,, \tag{15}$$

$$\nabla_{S,P} = \frac{\boldsymbol{e}_\lambda}{a\cos\phi_P}\frac{\partial}{\partial\lambda_{S,P}} + \frac{\boldsymbol{e}_\phi}{a}\frac{\partial}{\partial\phi_{S,P}}\,, \tag{16}$$

$$\Delta_{S,P} = \frac{1}{a^2\cos^2\phi_P}\left(\frac{\partial^2}{\partial{\lambda_{S,P}}^2} + \cos\phi_P\frac{\partial}{\partial\phi_{S,P}}\left(\cos\phi_P\frac{\partial}{\partial\phi_{S,P}}\right)\right)\,, \tag{17}$$

$$\nabla_{S,P}\cdot\boldsymbol{u} = \frac{1}{a\cos\phi_P}\left(\frac{\partial u}{\partial\lambda_{S,P}} + \frac{\partial v\cos\phi_P}{\partial\phi_{S,P}}\right)\,, \tag{18}$$

$$\boldsymbol{e}_r\cdot(\nabla_{S,P}\times\boldsymbol{u}) = \frac{1}{a\cos\phi_P}\left(\frac{\partial v}{\partial\lambda_{S,P}} - \frac{\partial u\cos\phi_P}{\partial\phi_{S,P}}\right)\,, \tag{19}$$

where $\boldsymbol{u} = \boldsymbol{e}_\lambda u + \boldsymbol{e}_\phi v$ and $\boldsymbol{e}_\lambda, \boldsymbol{e}_\phi, \boldsymbol{e}_r$ denote the unit vectors in spherical coordinates. Note that we do not need to make the traditional β-plane approximation for the Coriolis parameter f, since its full variations are resolved by the planetary scale coordinate ϕ_P.

2) Key steps of the expansion

We substitute the ansatz (9) in the governing equations (2) - (7) and collect terms of the same order in ε. Following DK we assume a radiative heating rate of about 1 K/day, this implies for the diabatic source term: $S_\theta \sim \mathcal{O}(\varepsilon^5)$. The magnitude of the friction source terms is estimated as: $S_{u,v} \sim \mathcal{O}(\varepsilon^2)$, if a relaxation time scale for the frictional effects of about 1 day is assumed. Source terms of this strength will induce leading order synoptic tendencies in the momentum equation.

(i) Vertical momentum balance

The expansion of the vertical momentum equation shows that the pressure and the density are hydrostatically balanced up to $\mathcal{O}(\varepsilon^4)$. If we make use of the ideal gas law (7) and of the Newtonian limit (which states that $\gamma - 1 = \mathcal{O}(\varepsilon)$ as $\varepsilon \to 0$), we obtain from the leading two orders hydrostatic balance (see Klein and Majda (2006) and DK for details): $p^{(0)} = \rho^{(0)} = \exp(-z)$ and $p^{(1)} = \rho^{(1)} = 0$. The next two orders of hydrostatic balance can be expressed as

$$\mathcal{O}\big(\varepsilon^2\big): \qquad \Theta^{(2)} = \frac{\partial}{\partial z}\pi^{(2)}\,, \tag{20}$$

$$\mathcal{O}\big(\varepsilon^3\big): \qquad \Theta^{(3)} = \frac{\partial}{\partial z}\pi^{(3)}\,, \tag{21}$$

where $\pi^{(i)} = p^{(i)}/\rho^{(0)}$.

(ii) Horizontal momentum balance

The leading order horizontal pressure variations on the planetary scale are described by $\pi^{(2)}$, consistent with the assumption (13) on $\Theta^{(2)}$. Further, the leading order synoptic scale horizontal pressure fluctuations are assumed an order of ε smaller and are modeled by $\pi^{(3)}$. If we allow for a dependence of $\pi^{(2)}$ on the synoptic scales, the horizontal pressure gradient $\nabla_S \pi^{(2)}$ will appear in the $\mathcal{O}(1)$ momentum equation. A pressure gradient of this strength must be balanced by a Coriolis force, which involves a velocity field scaled as $\varepsilon^{-1} u_{ref}$ (the leading order velocity $\boldsymbol{u}^{(0)}$ in the current asymptotic expansion (9) describes dimensional velocities of the order u_{ref}). Thus, the synoptic scale variations of $\pi^{(2)}$ imply unrealistic large synoptic scale velocities, such variations are inconsistent with the QG scaling and will not be considered here. With the consideration above, together with the result $w^{(0)} = 0$ from iii) below, we obtain that $\boldsymbol{u}^{(0)}$ is geostrophically balanced with respect to the pressure gradient on the synoptic (∇_S) and on the planetary scale (∇_P)

$$\mathcal{O}(\varepsilon): \qquad f\boldsymbol{e}_r \times \boldsymbol{u}^{(0)} = -\nabla_S \pi^{(3)} - \nabla_P \pi^{(2)}\,. \tag{22}$$

Since $\pi^{(2)}$ and f do not depend on the synoptic scales, (22) implies that the synoptic scale divergence of $\boldsymbol{u}^{(0)}$ disappears

$$f\nabla_S \cdot \boldsymbol{u}^{(0)} = 0\,. \tag{23}$$

The evolution of the velocity field $\boldsymbol{u}^{(0)}$ on the synoptic time scale appears in the next order equation

$$\mathcal{O}(\varepsilon^2): \qquad \frac{\partial}{\partial t_S}\boldsymbol{u}^{(0)} + \boldsymbol{u}^{(0)} \cdot \nabla_S \boldsymbol{u}^{(0)} + f\boldsymbol{e}_r \times \boldsymbol{u}^{(1)} = -\nabla_S \pi^{(4)} - \nabla_P \pi^{(3)} + \boldsymbol{S}_{\boldsymbol{u}}^{(2)}\,. \tag{24}$$

As in the case of the single scale PR from DK we proceed in the asymptotic expansion up to the $\mathcal{O}(\varepsilon^3)$ momentum equation

$$\begin{aligned}\mathcal{O}(\varepsilon^3): \qquad & \frac{\partial}{\partial t_S}\boldsymbol{u}^{(1)} + \frac{\partial}{\partial t_P}\boldsymbol{u}^{(0)} + \boldsymbol{u}^{(0)} \cdot \nabla_S \boldsymbol{u}^{(1)} + \boldsymbol{u}^{(1)} \cdot \nabla_S \boldsymbol{u}^{(0)} \\ & + \boldsymbol{u}^{(0)} \cdot \nabla_P \boldsymbol{u}^{(0)} + w^{(3)}\frac{\partial}{\partial z}\boldsymbol{u}^{(0)} + f\boldsymbol{e}_r \times \boldsymbol{v}^{(2)} - \boldsymbol{e}_\lambda \frac{u^{(0)}v^{(0)}\tan\phi_P}{a} \\ & + \boldsymbol{e}_\phi \frac{u^{(0)}u^{(0)}\tan\phi}{a} = -\nabla_P \pi^{(4)} + \frac{\rho^{(2)}}{\rho^{(0)}}\nabla_P \pi^{(2)} - \nabla_S \pi^{(5)} + \frac{\rho^{(2)}}{\rho^{(0)}}\nabla_S \pi^{(3)} + \boldsymbol{S}_{\boldsymbol{u}}^{(3)}\,.\end{aligned} \tag{25}$$

Comparing the last equation with the corresponding equation from DK, we note the additional terms due to the synoptic scale variations, e.g., the synoptic scale tendency of $\boldsymbol{u}^{(1)}$ $\left(\frac{\partial}{\partial t_S}\boldsymbol{u}^{(1)}\right)$ or the synoptic scale advection of $\boldsymbol{u}^{(1)}$ by $\boldsymbol{u}^{(0)}$ $\left(\boldsymbol{u}^{(0)} \cdot \nabla_S \boldsymbol{u}^{(1)}\right)$.

(iii) Continuity equation

The leading three orders in the mass conservation expansion give $w^{(0)} = w^{(1)} = w^{(2)} = 0$ (see DK for details). The $\mathcal{O}(\varepsilon^3)$ order equation reads

$$\mathcal{O}(\varepsilon^3): \qquad \nabla_S \cdot \rho^{(0)}\boldsymbol{u}^{(1)} + \nabla_P \cdot \rho^{(0)}\boldsymbol{u}^{(0)} + \frac{\partial}{\partial z}\rho^{(0)}w^{(3)} = 0\,. \tag{26}$$

Here the synoptic scale divergence of $\boldsymbol{u}^{(1)}$ (interpreted in the classical QG theory as the divergence due to the ageostrophic velocities) appears in the same order as the planetary scale divergence of the leading order wind field $\boldsymbol{u}^{(0)}$. Making use of (23), the next two orders in the continuity equation take the form

$$\mathcal{O}(\varepsilon^4): \qquad \nabla_S \cdot \rho^{(0)} \boldsymbol{u}^{(2)} + \nabla_P \cdot \boldsymbol{u}^{(1)} \rho^{(0)} + \frac{\partial}{\partial z} \rho^{(0)} w^{(4)} = 0\,, \tag{27}$$

$$\begin{aligned} \mathcal{O}(\varepsilon^5): \qquad & \frac{\partial}{\partial t_S} \rho^{(3)} + \nabla_S \cdot \boldsymbol{u}^{(0)} \rho^{(3)} + \nabla_S \cdot \boldsymbol{u}^{(1)} \rho^{(2)} + \nabla_S \cdot \boldsymbol{u}^{(3)} \rho^{(0)} \\ & + \frac{\partial}{\partial t_P} \rho^{(2)} + \nabla_P \cdot \boldsymbol{u}^{(0)} \rho^{(2)} + \nabla_P \cdot \boldsymbol{u}^{(2)} \rho^{(0)} \\ & + \frac{\partial}{\partial z} \left(\rho^{(0)} w^{(5)} + \rho^{(2)} w^{(3)} \right) = 0\,. \end{aligned} \tag{28}$$

(iv) Potential temperature equation

From the expansion of the potential temperature equation we have

$$\begin{aligned} \mathcal{O}(\varepsilon^5): \qquad & \frac{\partial}{\partial t_S} \Theta^{(3)} + \boldsymbol{u}^{(0)} \cdot \nabla_S \Theta^{(3)} + \frac{\partial}{\partial t_P} \Theta^{(2)} + \boldsymbol{u}^{(0)} \cdot \nabla_P \Theta^{(2)} \\ & + w^{(3)} \frac{\partial}{\partial z} \Theta^{(2)} = S_\Theta^{(5)}\,. \end{aligned} \tag{29}$$

It is worth to compare this result with the corresponding QG equation. In the latter theory $\Theta^{(2)}$ is interpreted as a horizontally uniform background temperature distribution and all terms involving it, except the stratification term, are set to zero. Here we consider the variations on the planetary spatial and temporal scales of $\Theta^{(2)}$ and their influence on the synoptic scale dynamics of $\Theta^{(3)}$.

b. Vorticity equation for the two scale PR

In this section we proceed with a derivation of a vorticity equation for the two scale model. Applying $-\frac{1}{a\cos\phi_P}\frac{\partial}{\partial\phi_S}\cos\phi_P$ to the $\boldsymbol{e}_\lambda$-component of (24) and $\frac{1}{a\cos\phi_P}\frac{\partial}{\partial\lambda_S}$ to the $\boldsymbol{e}_\phi$-component of (24), we obtain

$$\begin{aligned} & \frac{\partial}{\partial t_S} \zeta^{(0)} + \boldsymbol{u}^{(0)} \cdot \nabla_S \zeta^{(0)} + f \nabla_S \cdot \boldsymbol{u}^{(1)} \\ = & \frac{1}{a^2 \cos\phi_P} \frac{\partial}{\partial \phi_S} \frac{\partial}{\partial \lambda_P} \pi^{(3)} - \frac{1}{a^2 \cos\phi_P} \frac{\partial}{\partial \lambda_S} \frac{\partial}{\partial \phi_P} \pi^{(3)} + S_\zeta\,, \end{aligned} \tag{30}$$

where

$$\zeta^{(0)} = \boldsymbol{e}_r \cdot \nabla_S \times \boldsymbol{u}^{(0)} = \frac{1}{f}\Delta_S \pi^{(3)}\,, \tag{31}$$

$$S_\zeta = \boldsymbol{e}_r \cdot \nabla_S \times \boldsymbol{S}_{\boldsymbol{u}}^{(2)}\,. \tag{32}$$

With the help of (22) we can write for the planetary scale divergence of $\boldsymbol{u}^{(0)}$

$$f\nabla_P \cdot \boldsymbol{u}^{(0)} = -\frac{1}{a^2\cos\phi_P}\frac{\partial}{\partial\phi_S}\frac{\partial}{\partial\lambda_P}\pi^{(3)} + \frac{1}{a^2\cos\phi_P}\frac{\partial}{\partial\lambda_S}\frac{\partial}{\partial\phi_P}\pi^{(3)} - \beta v^{(0)}\,. \tag{33}$$

Thus, the two scale vorticity equation reads

$$\frac{\partial}{\partial t_S}\zeta^{(0)} + \boldsymbol{u}^{(0)} \cdot \nabla_S \zeta^{(0)} + f\nabla_P \cdot \boldsymbol{u}^{(0)} + f\nabla_S \cdot \boldsymbol{u}^{(1)} + \beta v^{(0)} = S_\zeta\,. \tag{34}$$

c. *Averaging over the synoptic scales*

Eq. (34) is not closed since it contains the unknown velocity corrections $\boldsymbol{u}^{(1)}$. They can be eliminated in a way similar to that encountered in the classical QG theory, see also Pedlosky (1984). This leads to two scale PR model equations describing the planetary and the synoptic scale dynamics; the model is summarized in the next section. A key step in the derivation is to split all variables into a synoptic scale average and a deviation from this average. In the case of the variable $\pi^{(3)}$ we obtain

$$\pi^{(3)}(\boldsymbol{X}_S, \boldsymbol{X}_P, z) = \pi_P^{(3)}(\boldsymbol{X}_P, z) + \pi_S^{(3)}(\boldsymbol{X}_S, \boldsymbol{X}_P, z)\,, \tag{35}$$

with

$$\pi_P^{(3)} = \overline{\pi^{(3)}}^S\,, \tag{36}$$

$$\overline{\pi_S^{(3)}}^S = 0\,, \tag{37}$$

where the averaging operator $\overline{()}^S$ denotes averaging over the synoptic spatial and temporal scales. Consequently, we can write for the leading order horizontal wind

$$\boldsymbol{u}^{(0)} = \underbrace{\frac{1}{f}\boldsymbol{e}_r \times \nabla_S \pi_S^{(3)}}_{=:\,\boldsymbol{u}_S^{(0)}} + \underbrace{\frac{1}{f}\boldsymbol{e}_r \times \nabla_P \pi^{(2)}}_{=:\,\boldsymbol{u}_P^{(0)}}\,. \tag{38}$$

Note that the synoptic scale wind field $\boldsymbol{u}_S^{(0)}$ is a function of the synoptic and planetary scales but the planetary scale wind field $\boldsymbol{u}_P^{(0)}$ of the planetary scales only and we have

$$\overline{\boldsymbol{u}_S^{(0)}}^{S} = 0\,. \tag{39}$$

The complete derivation of the two scale PR model is presented in appendix A and B.

4. Summary and discussion of the two scale PR model

Using a two scale asymptotic ansatz, we extended in a systematic way the region of validity of the planetary scale model from DK to the synoptic spatial and temporal scales. The model presented here relies on the assumption that the variations of the background stratification are comparable in magnitude with those adopted in the classical QG theory. The model equations are summarized below, for convenience of notation the superscripts indicating asymptotic expansion orders are dropped.

1) Planetary scale model

$$\left(\frac{\partial}{\partial t_P} + \boldsymbol{u}_P \cdot \nabla_P + w_P \frac{\partial}{\partial z}\right) \frac{f}{\rho_0} \frac{\partial \Theta}{\partial z} = S_{\frac{\partial \Theta}{\partial z}}\,, \tag{40}$$

$$\frac{\partial}{\partial t_P} \left(\frac{\partial}{\partial \tilde{y}_P} \frac{1}{f} \frac{\partial}{\partial y_P} \overline{P}^{z} - \frac{\beta}{f^2} \frac{\partial}{\partial y_P} \overline{P}^{z} - f \overline{P}^{z} \right) - \frac{\partial}{\partial \tilde{y}_P} N + \frac{\beta}{f} N = S_p\,, \tag{41}$$

$$N = \frac{\partial}{\partial \tilde{y}_P} \overline{\rho_0 \left(v_P u_P + \underline{\underline{v_S u_S}} \right)}^{S,\lambda_P,z} - \frac{\tan \phi_P}{a} \overline{\rho_0 \left(v_P u_P + \underline{\underline{v_S u_S}} \right)}^{S,\lambda_P,z} + \overline{\frac{\partial}{\partial z} P \frac{\partial}{\partial x_P} \frac{P}{\rho_0}}^{\lambda_P,z}\,, \tag{42}$$

$$\boldsymbol{u}_P = \frac{1}{f \rho_0} \boldsymbol{e}_r \times \nabla_P P\,, \quad \frac{\partial}{\partial z} \frac{P}{\rho_0} = \Theta\,, \quad \nabla_P \cdot \rho_0 \boldsymbol{u}_P + \frac{\partial}{\partial z} \rho_0 w_P = 0\,. \tag{43}$$

2) Synoptic scale model

$$\left(\frac{\partial}{\partial t_S} + \left(\boldsymbol{u}_S + \underline{\underline{\boldsymbol{u}_P}}\right) \cdot \nabla_S\right) q + \beta v_S + \frac{f}{\rho_0} \boldsymbol{u}_S \cdot \underline{\underline{\frac{\partial}{\partial z} \frac{\nabla_P \rho_0 \Theta}{\frac{\partial \Theta}{\partial z}}}} = S_q \,, \tag{44}$$

$$q = \frac{1}{f} \Delta_S \frac{p}{\rho_0} + \frac{f}{\rho_0} \frac{\partial}{\partial z} \left(\frac{\rho_0}{\frac{\partial \Theta}{\partial z}} \frac{\partial}{\partial z} \frac{p}{\rho_0} \right) \,, \quad \boldsymbol{u}_S = \frac{1}{f \rho_0} \boldsymbol{e}_r \times \nabla_S p \,. \tag{45}$$

The underlined terms, discussed below in details, describe planetary-synoptic interactions and we have used the notation

$$P = p^{(2)} \,, \quad p = p^{(3)} \,, \quad \Theta = \Theta^{(2)} \,, \quad \rho_0 = \rho^{(0)} \,, \quad w_p = \overline{w^{(3)}}^S \,, \tag{46}$$

$$\frac{\partial}{\partial x_P} = \frac{1}{a \cos \phi_P} \frac{\partial}{\partial \lambda_P} \,, \quad \frac{\partial}{\partial y_P} = \frac{1}{a} \frac{\partial}{\partial \phi_P} \,, \quad \frac{\partial}{\partial \tilde{y}_P} = \frac{1}{a \cos \phi_P} \frac{\partial}{\partial \phi_P} \cos \phi_P \,. \tag{47}$$

Equations (40)-(43) describe the planetary scale dynamics and (44)-(45) – the synoptic scale dynamics. The model equations include two advection equations (40), (44) for a PV type quantity and an evolution equation for the barotropic component of the background pressure (41), derived after applying the sublinear growth condition.

If we leave the planetary scales dependence of the variables out, equations (40), (41) reduce trivially and the underlined terms in (44) vanish. In this case (44) is the classical PV equation from the QG theory. On the other hand, if we assume that the variables do not depend on the synoptic scales, the interaction terms in (41), (42) vanish and (40) remains unchanged: thus we have the single scale planetary model from DK.

In the general case, when both synoptic and planetary scales are included, equations (40), (41) and (44) provide the planetary scale structure of Θ, $\overline{P}^z$ and the synoptic scale structure of p. The variable Θ characterizes the background stratification. But whereas in the classical QG model a horizontally uniform stratification is assumed, here it is governed by the evolution equation (40). Another difference to the QG theory is that we do not utilize a β-plane approximation in the derivation of the synoptic scale model (44). In the last model variation of the Coriolis parameter f (as well as β) on a planetary length scale are allowed. Equations (40) and (43) constitute the PGEs. As discussed in DK they do not represent a closed system, since a boundary condition for the surface pressure, or equivalently for the vertically averaged (barotropic component) pressure, is required. The latter is determined by the planetary barotropic vorticity equation (41). It is shown (see appendix B), that as in the single-scale PR the barotropic component of the background pressure $\overline{P}^z$ is zonally symmetric. This is in accordance with the observational evidence that leading modes of atmospheric variability, i.e., the NAM and SAM, are zonally symmetric and barotropic. Thus, (41) has the potential to describe the dynamics of zonally symmetric low-frequency modes.

The two underlined terms in (44) describe interactions between the planetary and the synoptic scales, or more precisely the influence of the planetary scale variations of the background pressure/temperature distribution on the synoptic scale PV field. The first term can be interpreted as the advection of synoptic scale PV by the planetary scale velocity field, the second as the interaction of synoptic velocities with PV gradient afforded by the planetary scale field. It is important to note that the latter PV includes only a stretching vorticity part, since the contribution from the relative vorticity (due to planetary scale velocity field) is an order of magnitude smaller in the asymptotic analysis. We observe that the barotropic model of Luo (2005) contains such additional interaction term (see eq. (2b) in Luo (2005)). We speculate that this results from the fact that the latter author starts his asymptotic analysis from the equivalent barotropic vorticity equation, which itself is derived under the quasi-geostrophic scaling. We observe further, that the model for the synoptic dynamics (44) reduces to the model of Pedlosky (1984), if we set ρ_0 to one and consider plane geometry.

It is important to note that from the equations describing the planetary scale dynamics only eq. (41), but not eq. (40), contains a feedback from the synoptic scale (see the underlined terms in (42)). We consider the first underlined term in (42), after applying the chain rule it will give rise in (41) to a term of the form $\frac{\partial}{\partial \tilde{y}_P}(v_S(-\frac{\partial}{\partial \tilde{y}_P}u_S))$. The latter term can be interpreted as a planetary meridional gradient of a relative vorticity flux, where the vorticity results from the planetary scale dependence of u_S. Such fluxes will directly affect the barotropic component of the background pressure. The background temperature Θ, on the other hand, will be influenced only indirectly by the synoptic scales through the barotropic part of the flow: changes in the background pressure imply changes in the planetary scale wind $\boldsymbol{u}_P$ and hence the temperature advection in (40) will be affected. Such type of feedback mechanism from the synoptic to the planetary scale is absent in the Pedlosky (1984) model and differs from the one proposed by Grooms et al. (2011). The latter author shows that for some anisotropic regimes (requiring either an anisotropy in the large-scale spatial coordinates or anisotropy in the large- and small-scale velocity fields) the planetary scale motion can be influenced by the synoptic scale at leading order through eddy buoyancy fluxes. This does not contradict our results, since the barotropic component of the flow was ommited in the analysis of Grooms et al. (2011) and the PR is not characterized by an anisotropy. Further, we observe that eq.(41) does not contain vertical advection and twisting terms. This is in accordance with budget analysis of low-frequency life-cycle studies (Cai and van den Dool 1994; Feldstein 1998, 2002), which found that the corresponding terms are small and spatially incoherent. We note that terms multiplied by β in (41) result from the advection of planetary vorticity by the ageostrophic flow (see appendix B). This is consistent with the analysis of Cai and van den Dool (1994): they found that such an advection is important for the very longest low-frequency wave.

5. Balances on the Planetary and Synoptic Scales in Numerical Experiments

In this section we address the question how closely the reduced planetary-synoptic asymptotic model captures the dynamics of a more complete fluid-dynamical model of the atmosphere. For that purpose we perform simulations with a model based on the primitive equations (PEs). Since the PEs are derived from the full compressible flow equations by assuming only a small aspect ratio of the vertical to horizontal length scale and the traditional approximation, these equations are much more comprehensive than the asymptotic model and apply to a wider range of scales. From the simulations with the PEs model we study the balances in the vorticity transport on the planetary and synoptic scale and compare them with the reduced asymptotic equations.

a. Model description

The numerical simulations are performed with the Portable University Model of the Atmosphere (PUMA; Fraedrich et al. 1998), which is a simplified global circulation model used for idealized experiments (e.g., Franzke 2002; Kleidon et al. 2003). It solves the PEs on a sphere for a dry ideal gas with diabatic and dissipation effects linearly parameterized through Newtonian cooling and Rayleigh friction (Held and Suarez 1994). The balance in the model vorticity transport can be written in pressure coordinates as

$$\frac{\partial}{\partial t}\zeta + \nabla \cdot \boldsymbol{u}(\zeta + f) + \boldsymbol{e}_r \cdot \nabla \times \left(\omega \frac{\partial}{\partial p}\boldsymbol{u}\right) + \frac{\zeta}{\tau_F} + K(-1)^h \nabla^{2h}\zeta = R\,, \tag{48}$$

where ζ denotes the relative vorticity, f the planetary vorticity, $\boldsymbol{u}$ the horizontal velocity vector, ω the vertical velocity and R the residuum due to errors in the interpolation of the fields from σ to pressure levels (the PUMA model equations use a σ-vertical coordinate). Further, we have the friction relaxation time scale τ_f and the hyperdiffusion coefficient K. All model variables are nondimensionalized using Ω and a^*.

We performed simulations with realistic orography as well as with an aquaplanet as lower boundary condition. The model was run at a T21 horizontal resolution, with 10 vertical σ-levels and with a time step of 30 min. For the analysis an output over 11 years with 12 h time increment was used, the first one year is ignored so as to not mis-interpret any spin up effects. We used the default value of 70 K for the equator to pole temperature difference in the restoration temperature profile and the seasonal cycle in the model was switched off.

The inspection of the orography run shows that PUMA is able to produce key features of the atmospheric circulation reasonably well for a simplified atmospheric model. At mid-latitudes a pronounced wavenumber 6, 7 structure with a period of ca. 8 days is visible over most of the simulation time. This wave implies a characteristic length scale of ~ 2000 km for the individual synoptic eddies, its time period is overestimated compared with the real atmosphere where the maximum of the synoptic activity lies around 4 days (Fig. 1). The time mean 500 hPa geopotential height shows, that the model reproduces the trough over Eastern Asia, but it shifts the trough over Canada to Greenland. The weak trough over Western Asia is absent in the model but a weak minimum over the Aleutian islands is visible. In the real atmosphere the depression over these islands is confined to the lower troposphere only. An explanation of these discrepancies can be the absence of land-sea thermal forcing in the model.

b. The two-scale PR in simulations

In this subsection we analyze the magnitudes of the different terms in the PUMA vorticity equation and compare the leading order balances with the two scale PR model. Recall the leading two orders of the vorticity equation (see (23), (34)) in the PR model

$$f\nabla_S \cdot \boldsymbol{u}^{(0)} = 0\,, \tag{49}$$

$$\frac{\partial}{\partial t_S}\zeta^{(0)} + \boldsymbol{u}^{(0)} \cdot \nabla_S \zeta^{(0)} + f\nabla_P \cdot \boldsymbol{u}^{(0)} + f\nabla_S \cdot \boldsymbol{u}^{(1)} + \beta v^{(0)} = 0\,. \tag{50}$$

Here all frictional source terms are dropped, since we analyse PUMA simulations at vertical levels in the free atmosphere well above the planetary boundary layer. Next, the results for the balances in the PUMA vorticity transport on the synoptic and planetary scales are presented.

1) Synoptic scale dynamics

The power spectral density of various terms in the model equation (48) as a function of zonal wavenumber and frequency is presented in Fig. 3 and 4. From the plots it is visible that the terms $f\frac{\partial \boldsymbol{u}}{\partial \lambda}$, $\frac{\partial \zeta}{\partial t}$ and βv show two pronounced maxima. The first maxima is at zonal wavenumber k=6 (k=6,7 for $f\frac{\partial \boldsymbol{u}}{\partial \lambda}$) and has a period around 8 d; the second maxima is at k=5 and period between 9 and 10 d. This structure resembles the two peaks associated with synoptic activity found in observational data, see Fig. 1. Further, in the power density of $f\frac{\partial \boldsymbol{u}}{\partial \lambda}$ and βv there is a hint of an isolated maximum at k=1,2 and frequency close to zero. This maximum results from quasi-stationary Rossby waves forced by orography, because it is absent in the aquaplanet simulation.

In order to compare the magnitude of different terms in the vorticity balance on the synoptic scale, we computed the cumulative spectral density (sum over spectral density for some wavenumber/period interval) for zonal wavenumbers $4 \leq k \leq 8$ and periods 7 d $\leq T \leq 10$ d. The results for three different pressure levels are shown in Table 2. Overall, it can be stated, that first the terms $f\frac{\partial u}{\partial \lambda}$ and $f\frac{\partial v}{\partial \phi}$ dominate and have similar magnitude. Second, if we add these terms together (see Table 2 and the plots for $f\nabla\cdot\boldsymbol{u}$ in Fig. 3, 4), the resulting variations are one to two orders smaller than those of the individual terms, implying that they nearly balance. Both results are consistent with the leading order vorticity balance in the asymptotic analysis (49), which states that on the synoptic scales the leading order in the expansion for the wind is divergence free.

The next order vorticity balance (50) from the PR suggests that terms including vorticity tendency, relative vorticity advection, planetary vorticity advection and horizontal divergence (multiplied by f) are next in importance in the vorticity transport. Indeed Table 2 shows that $\frac{\partial \zeta}{\partial t}$, βv, $u\frac{\partial \zeta}{\partial \lambda}$, $v\frac{\partial \zeta}{\partial \phi}$ and $f\nabla\cdot\boldsymbol{u}$ are larger than terms involving advection by the vertical velocity ω or the dissipation term F_{fr}. However, the individual magnitudes of the first terms show variations within a wide range from 10^{-1} up to 10^{-3}. Clearly, the dissipation term F_{fr} is even one order smaller and at 300 hPa and 500 hPa is comparable with $-\frac{\partial}{\partial \phi}(\omega \frac{\partial}{\partial p} u)$. This justifies the neglect of the nonconservative source term in (50). We observe further, that the $\zeta \frac{\partial u}{\partial \lambda}$ and $\zeta \frac{\partial v}{\partial \phi}$ terms are comparable with $v \frac{\partial \zeta}{\partial \phi}$ in magnitude. However, if added together the first terms nearly balance similarly to the balance observed in $f \nabla \cdot \boldsymbol{u}$.

Table 3 shows that the spectral properties discussed so far are observed at different latitudes as well.

2) Planetary scale dynamics

As discussed in the previous subsection the vorticity equation (50) describes the leading order synoptic scale dynamics, however, this two-scale equation also takes into account planetary scale variations of the fields through the terms $f \nabla_P \cdot \boldsymbol{u}^{(0)}$ and $\beta v^{(0)}$. Thus, (50) can be used to study the leading order vorticity balance on the planetary scale and the effect of the synoptic scales on that balance. We average (50) over the synoptic spatio-temporal scales in order to obtain the net influence on the planetary scale motions. The resulting equation reads

$$\overline{\nabla_P \cdot f \boldsymbol{u}^{(0)}}^S = 0 \,, \tag{51}$$

which states that for planetary scale motions the planetary vorticity flux vanishes. Further, in (51) there is no contribution from the synoptic scale vorticity fluxes. This is because of the the sublinear growth condition, which requires

$$\overline{\nabla_S \cdot \boldsymbol{u}^{(0)} \zeta^{(0)}}^S = 0 \,. \tag{52}$$

Note, that an effect due to synoptic eddy fluxes first appears in the next asymptotic order, cf. with the planetary barotropic vorticity equation (41). Equations (51) and (52) motivated us to study the divergence of the f- and ζ-flux in the PEs model. They suggest the following leading order balance on planetary spatial and temporal scales: i) the terms $u \frac{\partial \zeta}{\partial \lambda}, v \frac{\partial \zeta}{\partial \phi}, \zeta \frac{\partial u}{\partial \lambda}$ and $\zeta \frac{\partial v}{\partial \phi}$ sum to zero up to next order asymptotic corrections ii) the terms $f \frac{\partial u}{\partial \lambda}, f \frac{\partial v}{\partial \phi}$ and βv

sum to zero up to next order asymptotic corrections. Therefore, we consider the standard deviation of the terms $\nabla \cdot \boldsymbol{u}\zeta$ and $\nabla \cdot \boldsymbol{u}f$ in the PEs simulation relative to the standard deviation of the individual terms entering in the definitions of $\nabla \cdot \boldsymbol{u}\zeta$ and $\nabla \cdot \boldsymbol{u}f$. In order to extract variations with particular zonal and meridional scale, we expand the data in spherical harmonics. Each harmonic has a total wavenumber n and zonal wavenumber k, the difference $n-k$ defines the so-called meridional wavenumber and gives number of nodes from pole to pole. Thus, modes with small n and k ($n \geq k$) describe variations on planetary spatial scales, in both zonal and meridional direction. On the other hand, if n, k or both become larger, the corresponding spherical harmonic will capture synoptic spatial scales as well.

The top plots in Fig. 5 depict the normalized standard deviation of the spectral coefficients for $\nabla \cdot \boldsymbol{u}\zeta$ as a function of the total wavenumber n, where the normalization factor is given by the mean over the standard deviation of the terms: $u\frac{\partial \zeta}{\partial \lambda}, v\frac{\partial \zeta}{\partial \phi}, \zeta\frac{\partial u}{\partial \lambda}$ and $\zeta\frac{\partial v}{\partial \phi}$. Thus, small values of normalized standard deviation indicate that the latter terms compensate. Clearly, this compensation is especially pronounced for total wavenumbers $n \leq 3$ at both pressure level. However, the transition between a regime with compensation and non-compensation is smooth.

The averaging operator in (52) includes, in addition to a spatial averaging, an averaging over the synoptic time scales as well. Because of this we applied a low-pass filter to the data (Blackmon 1976), filtering out the synoptic time scales and all other time scales with periods smaller than 10 d. The results for the normalized standard deviation of $\nabla \cdot \boldsymbol{u}\zeta$ are shown in the bottom plots of Fig. 5. The time filtering shifts the position of the maximum with roughly one total wavenumber to the left and reduces the standard deviation at higher n. However, for lower wavenumbers nearly no changes are observed compared to the unfiltered data, indicating that the large-scale spatial modes are dominated by long-period variations.

From (51) we expect that the divergence of planetary vorticity flux vanishes on the planetary spatial scales. This balance differs from the leading order result on the synoptic scale (49), which states that the divergence of the wind multiplied by f vanishes. The upper row plots in Fig. 6 display the normalized standard deviation of $\nabla \cdot f\boldsymbol{u}$ and $f\nabla \cdot \boldsymbol{u}$ for different total wavenumbers n. The term $\nabla \cdot f\boldsymbol{u}$ has similar distribution as the term $\nabla \cdot \boldsymbol{u}\zeta$ from Fig. 5: as n increases it increases monotonically up to a maximum and than declines, the smallest values correspond again to small n. The term $f\nabla \cdot \boldsymbol{u}$ has a different behavior: it decreases at the beginning until it saturates around some low, constant value. The saturation is reached around $n = 5$ and $n = 6$ for the 200 and 500 hPa pressure level, respectively. At this wavenumber the synoptic scale balance (49) is reached. From the graph of the $\nabla \cdot f\boldsymbol{u}$-term appears that the balance on the planetary scale (51) is satisfied for n=1,2 where the smallest values are reached and the curve is below the one for $f\nabla \cdot \boldsymbol{u}$. As in the case of $\nabla \cdot \boldsymbol{u}\zeta$, the transition between the planetary and synoptic regime in $\nabla \cdot f\boldsymbol{u}$ and $f\nabla \cdot \boldsymbol{u}$ is smooth.

The bottom plots in Fig. 6 show, that the application of a low-pass filter to the data does not change qualitatively the behavior of $\nabla \cdot f\boldsymbol{u}$ and $f\nabla \cdot \boldsymbol{u}$. The results reported in this section were also observed in an aquaplanet simulation.

6. Conclusions and Outlook

Using a two scale asymptotic ansatz, we extended in a systematic way the region of validity of the planetary scale model from DK to the synoptic spatial and temporal scales. The resulting multi-scale model is summarized in eqs. (40)-(45). Already Mak (1991) incorporated in the QG model spherical geometry by considering higher order terms, but his model is valid for motions characterized by length scales smaller than the planetary scale. The model presented here consists of two coupled parts – for the planetary and for the synoptic dynamics. This is different from the geostrophic potential vorticity model of Vallis (Vallis 1996; Mundt et al. 1997), which consists of a single PV equation valid on the planetary and on the synoptic scale. The latter model is derived by choosing an appropriate scaling, which allows both the limit for the QG model and the limit for the PGEs, whereas here we have applied a multi-scale asymptotic derivation. The two scale wave models of Luo (2005); Luo et al. (2007) assume a scale separation between planetary and synoptic motion only in zonal direction, here we considered a horizontally isotropic planetary scaling. A study with the asymptotic approach, as applied here, of anisotropic motions with planetary zonal scale, but meridionally confined to the synoptic scale, reveals a model which describes a coupling between the planetary evolution of the leading QG PV and the synoptic evolution of the first order PV corrections from the QG^{+1} model of Muraki et al. (1999) (details of this regime can be found in Dolaptchiev (2009)). The anisotropic multi-scale ocean model of Grooms et al. (2011) is another example for an anisotropic scaling of the large-scale coordinates (here the planetary coordinates): the meridional coordinate in this model resolves a planetary length scale, whereas the large-scale zonal coordinate resolves a scale between the planetary and the synoptic spatial scale. In the context of the atmosphere, the external Rossby deformation radius (Oboukhov scale) might be a natural choice for an intermediate large-scale length scale between the planetary and synoptic scale. Such scale is relevant for atmospheric blockings and within the present asymptotic approach it can be accessed in a systematic way.

Equations (40) and (44) represent the anelastic analogon of Pedlosky's two scale model for the large-scale oceanic circulation (Pedlosky 1984). In his study Pedlosky (1984) applied an asymptotic expansion in two small parameters: one is the Rossby number and the other is the ratio between the synoptic and the planetary length scale. For the derivation of his model he considered the case when the ratio between the two small parameters is of the order one. Expressing in terms of ε Pedlosky's expansion parameters for our setup, it can be shown that their ratio is again one, which means that we have considered the same distinguished limit. The analysis of Pedlosky starts from the incompressible equations on a plane, here we study the compressible ones on a sphere. Nevertheless, the model PV transport equations have the same structure and are identical if we set ρ_0 in (40), (44) to one and neglect the effects due to the spherical geometry. A fundamental difference is the absence of a counterpart to the barotropic vorticity equation (41) in Pedlosky's model. In the ocean the barotropic component of the planetary scale flow is determined, e.g., by prescribing the surface wind or by including some additional friction in the leading order momentum equation. This is not applicable to the atmosphere, since the surface winds should be a part of the solution and the frictional effects are much smaller than in the ocean.

The additional evolution equation for the barotropic component of the flow (41) provides the only feedback from the synoptic scale processes to the planetary scale flow in the form of momentum fluxes. No such feedback is contained in Pedlosky's model. This type of feedback mechanism on the planetary scale differs from the one recently proposed by Grooms et al. (2011), where the planetary scale motion is influenced by the synoptic scale through eddy buoyancy fluxes.

One possible application of the two scale PR model presented here, is its implementation in the atmospheric module of an earth system model of intermediate complexity (EMIC Claussen et al. 2002). The CLIMBER EMIC (Petoukhov et al. 2000) solves a type of the PGEs (40), (43), but it uses a temperature based diagnostic closure for the barotropic component of the flow. Here (41) represents a prognostic alternative, which may provide for more realistic increased large-scale, low-frequency variability in future implementations.

In EMICs the synoptic fluxes are often parameterized as a macroturbulent diffusion. In this context the model for the synoptic scale dynamics (44) can be regarded as a higher order closure. The solution of the additional evolution equation for the synoptic scales might be avoided by applying a stochastic mode reduction strategy (Majda et al. 2003; Franzke et al. 2005; Franzke and Majda 2006; Dolaptchiev et al. 2012). Using this strategy one can derive stochastic differential equations for some "slow" variables taking into account in a systematic manner the interactions from the "fast" variables. In the case of the two scale PR model, we have a natural separation between fast (synoptic) and slow (planetary) modes. Thus one might apply a stochastic mode reduction procedure to the reduced two scale model and derive a stochastic parameterization for the synoptic correlation terms in (41), which is consistent with the synoptic scale model (44). An alternative approach avoiding synoptic scale parameterization is followed by Luo (2005); Luo et al. (2007) in studies of blockings and NAO dynamics. The latter phenomena are considered as nonlinear initial value problems of planetary-synoptic interactions, this allows to assume a synoptic eddy forcing prior to the evolution of the planetary scale motion.

The reduced barotropic vorticity equation has the potential to provide a diagnostic tool for studying planetary scale low-frequency dynamics in GCM or in observations. A number of studies (Cai and van den Dool 1994; Feldstein 1998, 2002; Franzke 2002) on the life-cycle of atmospheric low-frequency anomalies utilize budget analysis with the streamfunction tendency equation. In particular, with such an analysis the importance of different interaction terms, e.g., interactions with the time mean flow or high- and low-frequency transients, can be assessed systematically. In this context, the asymptotic analysis presented here stresses the importance of the barotropic, zonally symmetric component of the flow for the low-frequency dynamics. Further, it identifies terms containing zonally and vertically averaged synoptic scale momentum fluxes (or planetary meridional gradients of such fluxes) as relevant planetary-synoptic interactions. Those terms can be evaluated from observational data or GCM simulations and might be used as a diagnostic tool in interaction studies. Thus, the reduced planetary scale barotropic vorticity equation provides an alternative framework to apply a budget analysis, when the growth and decay of zonally symmetric anomalies with a planetary meridional scale, e.g., NAM and SAM, are investigated. Such model might give new insights in the interactions between the different spatial scales. Those spatial interactions are studied in the literature (Cai and van den Dool 1994; Feldstein 1998, 2002; Franzke 2002) by splitting the flow into zonal average and its deviation, whereas in the present approach the planetary and synoptic scales are associated with different ranges in wavenumber space. Another application of the present model is to use it as a data driven planetary scale model, in a way similar to Feldstein (2002). In such a model the synoptic fluxes are prescribed from GCM simulation or observation and the effect on the planetary scale dynamics can be studied by solving the reduced model equations.

The analysis from section 5 of numerical simulations with a primitive equations model showed that the leading order balances in the vorticity transport are consistent with the two scale asymptotic model. In particular, we find that for modes with planetary spatial scales (modes corresponding to spherical harmonics with a total wavenumber ≤ 2) the horizontal fluxes of relative and planetary vorticity are nearly divergence free. However, the transition between planetary and synoptic regime is smooth in the primitive equations model. The comparison between the numerical experiments and the asymptotic models can be extended in the present framework by considering the thermodynamic equation or higher order balances on the planetary and synoptic scales. The asymptotic analysis revealed that some higher order terms involve corrections to the leading order wind. These corrections can be calculated from the model output by considering the divergent part of the wind.

In future we plan to solve the two scale PR model numerically. This raises the question about the model behavior in the tropics where f tends to zero. If no frictional effects are considered, the geostrophically balanced leading order wind has a singularity at the equator. However, the asymptotic analysis of Majda and Klein (2003) showed that the background temperature field in the tropics is horizontally uniform (also known as the weak temperature gradient approximation). This condition on the temperature implies a vanishing pressure gradient which compensates the growth due to f. In the case of the two scale PR model further analysis is required, this model should be matched in a systematic way to the intraseasonal planetary equatorial synoptic scale model of Majda and Klein (2003).

Acknowledgments.

The authors thank the reviewers for their comments and suggestions which helped to improve the draft version of the manuscript. S. D. is thankful to U. Achatz for useful discussions. This contribution is partially supported by Deutsche Forschungsgemeinschaft, Grant KL 611/14.

APPENDIX A

PV formulation of the two scale model

Using (33) and the continuity equation (26), (30) can be expressed as

$$\frac{\partial}{\partial t_S}\zeta^{(0)} + \boldsymbol{u}^{(0)} \cdot \nabla_S \zeta^{(0)} + \beta v^{(0)} = \frac{f}{\rho^{(0)}}\frac{\partial}{\partial z}\rho^{(0)} w^{(3)} + S_\zeta \,. \tag{A1}$$

Eliminating the vertical velocity with the help of (29), we have

$$\begin{aligned}\frac{\partial}{\partial t_S}\zeta^{(0)} + \boldsymbol{u}^{(0)} \cdot \nabla_S \zeta^{(0)} + \beta v^{(0)} = \\ -\frac{f}{\rho^{(0)}}\frac{\partial}{\partial z}\frac{\rho^{(0)}}{\frac{\partial}{\partial z}\Theta^{(2)}}\left(\frac{\partial}{\partial t_S}\Theta^{(3)} + \frac{\partial}{\partial t_P}\Theta^{(2)} + \boldsymbol{u}^{(0)} \cdot \nabla_S \Theta^{(3)} + \boldsymbol{u}^{(0)} \cdot \nabla_P \Theta^{(2)}\right) + S_{pv}\,,\end{aligned} \tag{A2}$$

where we have denoted all source terms due to diabatic and frictional effects with S_{pv}. In equation (A2) both the planetary and the synoptic scales are involved; we have reduced the unknown variables to two $\pi^{(2)}(\boldsymbol{X}_P, z)$ and $\pi^{(3)}(\boldsymbol{X}_S, \boldsymbol{X}_P, z)$, since $\boldsymbol{u}^{(0)}, \Theta^{(2)}, \Theta^{(3)}$ and $\zeta^{(0)}$ can be expressed in terms of them, see (22), (20), (21) and (31). Next, we derive two separate equations for the unknowns, as usual in the multiple scales asymptotic techniques this is achieved by applying the sublinear growth condition (see also Pedlosky (1984)).

Equation (A2) can be rewritten, with the terms depending on the planetary scales only appearing on the right hand side, as

$$\begin{aligned}\frac{\partial}{\partial t_S}q^{(3)} + \left(\boldsymbol{u}_S^{(0)} + \boldsymbol{u}_P^{(0)}\right) \cdot \nabla_S q^{(3)} + \beta v_S^{(0)} + \frac{f}{\rho^{(0)}}\boldsymbol{u}_S^{(0)} \cdot \frac{\partial}{\partial z}\frac{\nabla_P \rho^{(0)}\Theta^{(2)}}{\partial\Theta^{(2)}/\partial z} \\ -S_q = -\beta v_P^{(0)} - \frac{f}{\rho^{(0)}}\frac{\partial}{\partial z}\left(\frac{\rho^{(0)}}{\partial\Theta^{(2)}\partial z}\left(\frac{\partial}{\partial t_P}\Theta^{(2)} + \boldsymbol{u}_P^{(0)} \cdot \nabla_P \Theta^{(2)}\right)\right) + S_{\frac{\partial\Theta}{\partial z}}\,,\end{aligned} \tag{A3}$$

where

$$q^{(3)} = \frac{1}{f}\Delta_S \pi^{(3)} + \frac{f}{\rho^{(0)}}\frac{\partial}{\partial z}\left(\frac{\rho^{(0)}\partial\pi^{(3)}/\partial z}{\partial\Theta^{(2)}/\partial z}\right)\,. \tag{A4}$$

In eq.(A3) $S_{\frac{\partial\Theta}{\partial z}}$ represents the synoptic scale average of S_{pv} and S_q the deviations from this average. The advection terms on the rhs of (A3) can be written as the divergence of a flux

$$\begin{aligned}
&\frac{\partial}{\partial t_S}q^{(3)} + \nabla_S \cdot \left((\boldsymbol{u}_S^{(0)} + \boldsymbol{u}_P^{(0)})q^{(3)} + \frac{\beta \boldsymbol{e}_\lambda \pi^{(3)}}{f} - \frac{\boldsymbol{e}_z \pi^{(3)}}{\rho^{(0)}} \times \frac{\partial}{\partial z}\frac{\nabla_P \rho^{(0)}\Theta^{(2)}}{\partial\Theta^{(2)}/\partial z} \right) \\
&-S_q = -\beta v_P^{(0)} - \frac{f}{\rho^{(0)}}\frac{\partial}{\partial z}\left(\frac{\rho^{(0)}}{\partial\Theta^{(2)}\partial z}\left(\frac{\partial}{\partial t_P}\Theta^{(2)} + \boldsymbol{u}_P^{(0)} \cdot \nabla_P \Theta^{(2)} \right) \right) + S_{\frac{\partial\Theta}{\partial z}} \,.
\end{aligned} \tag{A5}$$

The lhs of (A5) vanishes after averaging the equation over the synoptic scales and applying the sublinear growth condition, but the rhs remains unchanged (since it does not depend on the synoptic scales). Thus both sides of (A5) have to vanish independently and we obtain from the lhs

$$\frac{\partial}{\partial t_S}q^{(3)} + \left(\boldsymbol{u}_S^{(0)} + \boldsymbol{u}_P^{(0)}\right) \cdot \nabla_S q^{(3)} + \beta v_S^{(0)} + \frac{f}{\rho^{(0)}}\boldsymbol{u}_S^{(0)} \cdot \frac{\partial}{\partial z}\frac{\nabla_P \rho^{(0)}\Theta^{(2)}}{\partial\Theta^{(2)}/\partial z} = S_q \,. \tag{A6}$$

The rhs of (A5) can be simplified further (see Dolaptchiev (2009) for the complete derivation)

$$\left(\frac{\partial}{\partial t_P} + \boldsymbol{u}_P^{(0)} \cdot \nabla_P + w_P \frac{\partial}{\partial z} \right) \frac{f}{\rho^{(0)}}\frac{\partial}{\partial z}\Theta^{(2)} = S_{\frac{\partial\Theta}{\partial z}} \,. \tag{A7}$$

where $w_P^{(3)} = \overline{w^{(3)}}^S$.

APPENDIX B

Evolution equation for the barotropic component of the pressure

As discussed in DK, the planetary scale PV eq. (A7) requires a closure for the vertically averaged pressure $p^{(2)}$ (barotropic component). Here we derive an evolution equation for that component in the two scale setup form section 2b. In order to see the net effect from the synoptic scales on the planetary scale pressure distribution, we have to average first the asymptotic equations form section 3 over the synoptic variables.

a. Averaging over the synoptic scales

(i) Continuity equation

$$\mathcal{O}(\varepsilon^3): \qquad \nabla_P \cdot \overline{\rho^{(0)}\boldsymbol{u}^{(0)}}^S + \frac{\partial}{\partial z}\overline{\rho^{(0)}w^{(3)}}^S = 0\,, \tag{B1}$$

$$\mathcal{O}(\varepsilon^4): \qquad \nabla_P \cdot \overline{\rho^{(0)}\boldsymbol{u}^{(1)}}^S + \frac{\partial}{\partial z}\overline{\rho^{(0)}w^{(4)}}^S = 0\,, \tag{B2}$$

$$\begin{aligned}\mathcal{O}(\varepsilon^5): \qquad & \frac{\partial}{\partial t_P}\rho^{(2)} + \nabla_P \cdot \overline{\boldsymbol{u}^{(0)}\rho^{(2)}}^S + \nabla_P \cdot \overline{\boldsymbol{u}^{(2)}\rho^{(0)}}^S \\ & + \frac{\partial}{\partial z}\left(\overline{\rho^{(0)}w^{(5)} + \rho^{(2)}w^{(3)}}^S\right) = 0\,.\end{aligned} \tag{B3}$$

We average vertically (B1), apply vanishing vertical velocity at the bottom and at the top of the domain as boundary condition and express the horizontal divergence with the help of eq. (33) to obtain

$$\frac{\beta}{f}\overline{\rho^{(0)}v^{(0)}}^{S,z} = 0\,. \tag{B4}$$

Consequently, the barotropic component of the pressure $p^{(2)}$ is zonally symmetric

$$\overline{p^{(2)}}^z = \overline{p^{(2)}}^z(\phi_P, t_P)\,. \tag{B5}$$

(ii) Potential temperature equation

Averaging over the potential temperature equation (29) and rewriting it in conservation form with the help of (B1), we have

$$\mathcal{O}(\varepsilon^5): \qquad \frac{\partial}{\partial t_P}\rho^{(0)}\Theta^{(2)} + \overline{\nabla_P \cdot \boldsymbol{u}^{(0)}\rho^{(0)}\Theta^{(2)}}^S + \frac{\partial}{\partial z}\overline{w^{(3)}\rho^{(0)}\Theta^{(2)}}^S = \overline{\rho^{(0)}S_\Theta^{(5)}}^S\,. \tag{B6}$$

(iii) Momentum equation

The equation for the $\boldsymbol{e}_\lambda$-component of (25) is written with (26) in conservation form, after averaging the result over the synoptic scales we have

$$
\begin{aligned}
\mathcal{O}(\varepsilon^3): \qquad & \frac{\partial}{\partial t_P}\rho^{(0)}\overline{u^{(0)}}^S + \nabla_P \cdot \overline{\boldsymbol{u}^{(0)}\rho^{(0)}u^{(0)}}^S + \frac{\partial}{\partial z}\overline{w^{(3)}\rho^{(0)}u^{(0)}}^S - f\overline{v^{(2)}}^S \\
& - \frac{\overline{u^{(0)}v^{(0)}\tan\phi_P}^S}{a} = -\frac{1}{a\cos\phi_P}\frac{\partial}{\partial\lambda_P}\overline{\pi^{(4)}}^S + \frac{\rho^{(2)}}{\rho^{(0)}}\frac{1}{a\cos\phi_P}\frac{\partial}{\partial\lambda_P}\overline{\pi^{(2)}}^S + \overline{\rho^{(0)}S_u^{(3)}}^S .
\end{aligned}
\tag{B7}
$$

Here we have used the sublinear growth condition (11) and the fact that $\boldsymbol{u}^{(0)}\cdot\nabla_S u^{(1)} = \nabla_S\cdot\boldsymbol{u}^{(0)}u^{(1)}$ because of (23).

b. *Derivation of the evolution equation for the planetary scale barotropic pressure*

We average the momentum eq. (B7), the temperature eq. (B6) and the continuity eq. (B3) over z and λ_P to obtain

$$
\overline{\rho^{(0)}v^{(2)}} = \frac{1}{f}\left\{\frac{\partial}{\partial t_P}\overline{\rho^{(0)}u^{(0)}} + \frac{\partial}{\partial\tilde{y}_P}\overline{v^{(0)}\rho^{(0)}u^{(0)}} - \overline{\rho^{(0)}u^{(0)}v^{(0)}}\frac{\tan\phi_P}{a} - \overline{\rho^{(2)}\frac{\partial}{\partial x_P}\pi^{(2)}} + \overline{\rho^{(0)}S_u^{(3)}}\right\},
\tag{B8}
$$

$$
\frac{\partial}{\partial t_P}\overline{\rho^{(0)}\Theta^{(2)}} + \frac{\partial}{\partial\tilde{y}_P}\overline{v^{(0)}\rho^{(0)}\Theta^{(2)}} = \overline{\rho^{(0)}S_\Theta^{(5)}},
\tag{B9}
$$

$$
\frac{\partial}{\partial\tilde{y}_P}\overline{\rho^{(0)}v^{(2)}} = -\frac{\partial}{\partial t_P}\overline{\rho^{(2)}} - \frac{\partial}{\partial\tilde{y}_P}\overline{v^{(0)}\rho^{(2)}}
\tag{B10}
$$

Here the overbar denotes an average over the synoptic scales, λ_P and z; $\frac{\partial}{\partial x_P}$ and $\frac{\partial}{\partial\tilde{y}_P}$ are defined in (47). The time derivative of $\rho^{(2)}$ in (B10) can be expressed with the help of (B9) in terms of $p^{(2)}$ only (see also eq.(73)-(77) from DK), thus we have

$$
\frac{\partial}{\partial\tilde{y}_P}\overline{\rho^{(0)}v^{(2)}} = -\frac{\partial}{\partial t_P}\overline{p^{(2)}} + \overline{\rho^{(0)}S_\Theta^{(5)}}
\tag{B11}
$$

Substituting (B8) in (B11), we have

$$\begin{aligned}
&\frac{\partial}{\partial t_P}\left(-\frac{\partial}{\partial \tilde{y}_P}\overline{u^{(0)}\rho^{(0)}} + \frac{\beta}{f}\overline{u^{(0)}\rho^{(0)}} - f\overline{p^{(2)}}\right) \\
&- \frac{\partial}{\partial \tilde{y}_P}\left\{\frac{\partial}{\partial \tilde{y}_P}\overline{v^{(0)}\rho^{(0)}u^{(0)}} - \frac{\overline{\rho^{(0)}u^{(0)}v^{(0)}}\tan\phi_P}{a} - \overline{\rho^{(2)}\frac{\partial}{\partial x_P}\pi^{(2)}}\right\} \\
&+ \frac{\beta}{f}\left\{\frac{\partial}{\partial \tilde{y}_P}\overline{v^{(0)}\rho^{(0)}u^{(0)}} - \frac{\overline{\rho^{(0)}u^{(0)}v^{(0)}}\tan\phi_P}{a} - \overline{\rho^{(2)}\frac{\partial}{\partial x_P}\pi^{(2)}}\right\} = S_p\,, \qquad \text{(B12)}
\end{aligned}$$

where S_p denotes the source terms entering the above equation. Finally, eq. (41) is obtained from (B12) after expressing the zonal wind $u^{(0)}$ entering the time derivative term in terms of the pressure $p^{(2)}$ using (38), (39) and (B5).

REFERENCES

Blackmon, M. L., 1976: A Climatological Spectral Study of the 500 mb Geopotential Height of the Northern Hemisphere. *J. Atmos. Sci.*, **33**, 1607–1623.

Cai, M. and H. M. van den Dool, 1994: Dynamical Decomposition of Low-Frequency Tendencies. *Journal of Atmospheric Sciences*, **51**, 2086–2100, doi:10.1175/1520-0469(1994)051⟨2086:DDOLFT⟩2.0.CO;2.

Charney, J. G., 1948: On the scale of atmospheric motion. *Geofys. Publ. Oslo*, **17**, 1–17.

Claussen, M., et al., 2002: Earth system models of intermediate complexity: closing the gap in the spectrum of climate system models. *Climate Dynamics*, **18**, 579–586, doi:10.1007/s00382-001-0200-1.

Dolaptchiev, S. I., 2009: Asymptotic models for planetary scale atmospheric motions. Ph.D. thesis, Freie Universität Berlin, http://www.diss.fu-berlin.de/diss.

Dolaptchiev, S. I., U. Achatz, and I. Timofeyev, 2012: Stochastic closure for local averages in the finite-difference discretization of the forced Burgers equation. *Theor. Comp. Fluid Dyn.*, doi:10.1007/s00162-012-0270-1.

Dolaptchiev, S. I. and R. Klein, 2009: Planetary geostrophic equations for the atmosphere with evolution of the barotropic flow. *Dynamics of Atmospheres and Oceans*, **46**, 46–61.

Feldstein, S., 1998: The Growth and Decay of Low-Frequency Anomalies in a GCM. *Journal of Atmospheric Sciences*, **55**, 415–428, doi:10.1175/1520-0469(1998)055⟨0415:TGADOL⟩2.0.CO;2.

Feldstein, S. B., 2002: Fundamental mechanisms of the growth and decay of the PNA teleconnection pattern. *Quarterly Journal of the Royal Meteorological Society*, **128**, 775–796, doi:10.1256/0035900021643683.

Fraedrich, K. and H. Böttger, 1978: A Wavenumber-Frequency Analysis of the 500 mb Geopotential at 50°N. *J. Atmos. Sci.*, **35**, 745–745.

Fraedrich, K. and E. Kietzig, 1983: Statistical Analysis and Wavenumber-Frequency Spectra of the 500 mb Geopotential along 50°S. *J. Atmos. Sci.*, **40**, 1037–1045.

Fraedrich, K., E. Kirk, and F. Lunkeit, 1998: Portable University Model of the Atmosphere. Tech. Rep. 16, DKRZ.

Franzke, C., 2002: Dynamics of Low-Frequency Variability: Barotropic Mode. *J. Atmos. Sci.*, **59**, 2897–2909.

Franzke, C. and A. J. Majda, 2006: Low-Order Stochastic Mode Reduction for a Prototype Atmospheric GCM. *J. Atmos. Sci.*, **63**, 457–479.

Franzke, C., A. J. Majda, and E. Vanden-Eijnden, 2005: Low-Order Stochastic Mode Reduction for a Realistic Barotropic Model Climate. *J. Atmos. Sci.*, **62**, 1722–1745.

Gall, R., 1976: A Comparison of Linear Baroclinic Instability Theory with the Eddy Statistics of a General Circulation Model. *J. Atmos. Sci.*, **33**, 349–373.

Grooms, I., K. Julien, and B. Fox-Kemper, 2011: On the interactions between planetary geostrophy and mesoscale eddies. *Dynamics of Atmospheres and Oceans*, **51**, 109–136, doi:10.1016/j.dynatmoce.2011.02.002.

Hayashi, Y. and D. G. Golder, 1977: Space-Time Spectral Analysis of Mid-Latitude Disturbances Appearing in a GFDL General Circulation Model. *J. Atmos. Sci.*, **34**, 237–262.

Held, I. M., 2005: The Gap between Simulation and Understanding in Climate Modeling. *Bulletin of the American Meteorological Society*, **86**, 1609–1614, doi:10.1175/BAMS-86-11-1609.

Held, I. M. and M. J. Suarez, 1994: A Proposal for the Intercomparison of the Dynamical Cores of Atmospheric General Circulation Models. *Bulletin of the American Meteorological Society, vol. 75, Issue 10, pp.1825-1830*, **75**, 1825–1830.

Hoskins, B. J., I. N. James, and G. H. White, 1983: The Shape, Propagation and Mean-Flow Interaction of Large-Scale Weather Systems. *J. Atmos. Sci.*, **40**, 1595–1612.

Kleidon, A., K. Fraedrich, T. Kunz, and F. Lunkeit, 2003: The atmospheric circulation and states of maximum entropy production. *Geophys. Res. Let.*, **30 (23)**, 230 000–1.

Klein, R., 2000: Asymptotic analyses for atmospheric flows and the construction of asymptotically adaptive numerical methods. *Zeitschr. Angew. Math. Mech.*, **80**, 765–770.

Klein, R., 2004: An applied mathematical view of theoretical meteorology. *Applied Mathematics Entering the 21st Century, invited talks at the ICIAM 2003 Conference*, J. Hill and R. Moore, Eds., SIAM proceedings in Applied Mathematic, Vol. 116.

Klein, R., 2008: An unified approach to meteorological modelling based on multiple-scales asymptotics. *Advances in Geosciences*, **15**, 23–33.

Klein, R. and A. J. Majda, 2006: Systematic multiscale models for deep convection on mesoscales. *Theoretical and Computational Fluid Dynamics*, **20**, 525–551.

Luo, D., 2005: A Barotropic Envelope Rossby Soliton Model for Block-Eddy Interaction. Part I: Role of Topography. *Journal of Atmospheric Sciences*, **62**, 5–21.

Luo, D., F. Huang, and Y. Diao, 2001: Interaction between antecedent planetary-scale envelope soliton blocking anticyclone and synoptic-scale eddies: Observations and theory. *J. Geoph. Res.*, **106**, 31 795–31 816, doi:10.1029/2000JD000086.

Luo, D., A. R. Lupo, and H. Wan, 2007: Dynamics of Eddy-Driven Low-Frequency Dipole Modes. Part I: A Simple Model of North Atlantic Oscillations. *Journal of Atmospheric Sciences*, **64**, 3–27, doi:10.1175/JAS3818.1.

Majda, A. and R. Klein, 2003: Systematic multi-scale models for the tropics. *J. Atmos. Sci.*, **60**, 393–408.

Majda, A. J., I. Timofeyev, and E. Vanden-Eijnden, 2003: Systematic Strategies for Stochastic Mode Reduction in Climate. *J. Atmos. Sci.*, **60**, 1705–1722.

Mak, M., 1991: Influence of the Earth's Sphericity in the Quasi-Geostrophic Theory. *Journal of Met. Soc. Japan*, **69**, 497–510.

Mundt, M., G. Vallis, and J. Wang, 1997: Balanced Models and Dynamics for the Large-and Mesoscale Circulation. *Jour. Phys. Ocean.*, **27**, 1133–1152.

Muraki, D. J., C. Snyder, and R. Rotunno, 1999: The Next-Order Corrections to Quasigeostrophic Theory. *J. Atmos. Sci.*, **56**, 1547–1560.

Owinoh, A. Z., B. Stevens, and R. Klein, 2011: Multiscale Asymptotics Analysis for the Mesoscale Dynamics of Cloud-Topped Boundary Layers. *Journal of Atmospheric Sciences*, **68**, 379–402, doi:10.1175/2010JAS3469.1.

Päschke, E., P. Marschalik, A. Z. Owinoh, and R. Klein, 2012: Motion and structure of atmospheric mesoscale baroclinic vortices: dry air and weak environmental shear. *Journal of Fluid Mechanics*, **701**, 137–170, doi:10.1017/jfm.2012.144.

Pedlosky, J., 1984: The Equations for Geostrophic Motion in the Ocean. *Jour. Phys. Ocean.*, **14**, 448–455.

Pedlosky, J., 1987: *Geophysical Fluid Dynamics*. 2d ed., Springer Verlag, New York.

Petoukhov, V., A. Ganopolski, V. Brovkin, M. Claussen, A. Eliseev, C. Kubatzki, and S. Rahmstorf, 2000: CLIMBER-2: A Climate System Model of Intermediate Complexity.

Part I: Model Description and Performance for Present Climate. *Climate Dynamics*, **16**, 1–17.

Phillips, N. A., 1963: Geostrophic Motion. *Reviews of Geophysics*, **1**, 123–175.

Robinson, A. and H. Stommel, 1959: The Oceanic Thermocline and the Associated Thermohaline Circulation. *Tellus*, **11**, 295–308.

Vallis, G. K., 1996: Potential vorticity inversion and balanced equations of motion for rotating and stratified flows. *Quarterly Journal of the Royal Meteorological Society*, **122**, 291–322.

Welander, P., 1959: An Advective Model for the Ocean Thermocline. *Tellus*, **11**, 309–318.

List of Tables

1 Scaling for the planetary and synoptic coordinates 40

2 Cumulative power spectral density for various terms in the vorticity equation (48) and at three different pressure levels. Shown is the sum over power density for zonal wavenumbers $4 \leq k \leq 8$ and periods $7 \text{ d} \leq T \leq 10 \text{ d}$ at 50°N in units of Ω^4. The following abbrevation is used: F_{fr} for the Rayleigh friction and hyperdiffusion terms ; $\frac{\partial}{\partial \lambda}$ for the zonal derivative $\frac{1}{\cos\phi}\frac{\partial}{\partial \lambda}$ and $\frac{\partial}{\partial \phi}$ for the meridional derivative $\frac{1}{\cos\phi}\frac{\partial \cos\phi}{\partial \phi}$, except for the operator in $v\frac{\partial \zeta}{\partial \phi}$. 41

3 Same as in table 2 but for different latitudes, all results for 300 hPa pressure level. 42

TABLE 1. Scaling for the planetary and synoptic coordinates

Coordinates:	synoptic	planetary
horizontal	$\lambda_S = \lambda/\varepsilon$	$\lambda_P = \lambda$
	$\phi_S = \phi/\varepsilon$	$\phi_P = \phi$
temporal	$t_S = \varepsilon^2 t$	$t_P = \varepsilon^3 t$

TABLE 2. Cumulative power spectral density for various terms in the vorticity equation (48) and at three different pressure levels. Shown is the sum over power density for zonal wavenumbers $4 \leq k \leq 8$ and periods $7\text{ d} \leq T \leq 10\text{ d}$ at 50°N in units of Ω^4. The following abbrevation is used: F_{fr} for the Rayleigh friction and hyperdiffusion terms ; $\frac{\partial}{\partial\lambda}$ for the zonal derivative $\frac{1}{\cos\phi}\frac{\partial}{\partial\lambda}$ and $\frac{\partial}{\partial\phi}$ for the meridional derivative $\frac{1}{\cos\phi}\frac{\partial\cos\phi}{\partial\phi}$, except for the operator in $v\frac{\partial\zeta}{\partial\phi}$.

200 hPa						
$f\frac{\partial u}{\partial\lambda}$	$f\frac{\partial v}{\partial\phi}$	$f\nabla\cdot\boldsymbol{u}$	$\frac{\partial\zeta}{\partial t}$	βv	$u\frac{\partial\zeta}{\partial\lambda}$	$v\frac{\partial\zeta}{\partial\phi}$
3.41e-01	3.54e-01	3.15e-02	1.46e-02	1.07e-02	1.86e-01	1.83e-03
$\zeta\frac{\partial u}{\partial\lambda}$	$\zeta\frac{\partial v}{\partial\phi}$	$\zeta\nabla\cdot\boldsymbol{u}$	$\frac{\partial}{\partial\lambda}(\omega\frac{\partial}{\partial p}v)$	$-\frac{\partial}{\partial\phi}(\omega\frac{\partial}{\partial p}u)$	F_{fr}	R
3.41e-03	3.39e-03	3.26e-04	2.45e-05	4.51e-05	1.90e-04	7.47e-05

300 hPa						
$f\frac{\partial u}{\partial\lambda}$	$f\frac{\partial v}{\partial\phi}$	$f\nabla\cdot\boldsymbol{u}$	$\frac{\partial\zeta}{\partial t}$	βv	$u\frac{\partial\zeta}{\partial\lambda}$	$v\frac{\partial\zeta}{\partial\phi}$
5.04e-01	5.46e-01	3.23e-02	2.25e-02	1.54e-02	2.27e-01	3.14e-03
$\zeta\frac{\partial u}{\partial\lambda}$	$\zeta\frac{\partial v}{\partial\phi}$	$\zeta\nabla\cdot\boldsymbol{u}$	$\frac{\partial}{\partial\lambda}(\omega\frac{\partial}{\partial p}v)$	$-\frac{\partial}{\partial\phi}(\omega\frac{\partial}{\partial p}u)$	F_{fr}	R
4.14e-03	4.32e-03	3.12e-04	5.51e-06	1.21e-04	3.24e-04	3.69e-05

500 hPa						
$f\frac{\partial u}{\partial\lambda}$	$f\frac{\partial v}{\partial\phi}$	$f\nabla\cdot\boldsymbol{u}$	$\frac{\partial\zeta}{\partial t}$	βv	$u\frac{\partial\zeta}{\partial\lambda}$	$v\frac{\partial\zeta}{\partial\phi}$
4.55e-01	5.07e-01	5.65e-03	2.40e-02	1.49e-02	1.23e-01	2.52e-03
$\zeta\frac{\partial u}{\partial\lambda}$	$\zeta\frac{\partial v}{\partial\phi}$	$\zeta\nabla\cdot\boldsymbol{u}$	$\frac{\partial}{\partial\lambda}(\omega\frac{\partial}{\partial p}v)$	$-\frac{\partial}{\partial\phi}(\omega\frac{\partial}{\partial p}u)$	F_{fr}	R
1.72e-03	1.87e-03	3.43e-05	1.02e-05	5.85e-04	3.45e-04	2.06e-05

Table 3. Same as in table 2 but for different latitudes, all results for 300 hPa pressure level.

40°N						
$f\frac{\partial u}{\partial\lambda}$	$f\frac{\partial v}{\partial\phi}$	$f\nabla\cdot\boldsymbol{u}$	$\frac{\partial\zeta}{\partial t}$	βv	$u\frac{\partial\zeta}{\partial\lambda}$	$v\frac{\partial\zeta}{\partial\phi}$
4.13e-01	4.62e-01	3.31e-02	2.01e-02	1.60e-02	2.51e-01	4.91e-03
$\zeta\frac{\partial u}{\partial\lambda}$	$\zeta\frac{\partial v}{\partial\phi}$	$\zeta\nabla\cdot\boldsymbol{u}$	$\frac{\partial}{\partial\lambda}(\omega\frac{\partial}{\partial p}v)$	$-\frac{\partial}{\partial\phi}(\omega\frac{\partial}{\partial p}u)$	F_{fr}	R
2.21e-03	2.52e-03	1.62e-04	2.88e-06	1.35e-04	2.15e-04	2.54e-05

60°N						
$f\frac{\partial u}{\partial\lambda}$	$f\frac{\partial v}{\partial\phi}$	$f\nabla\cdot\boldsymbol{u}$	$\frac{\partial\zeta}{\partial t}$	βv	$u\frac{\partial\zeta}{\partial\lambda}$	$v\frac{\partial\zeta}{\partial\phi}$
7.31e-01	6.02e-01	1.87e-02	1.67e-02	7.70e-03	1.17e-01	3.05e-03
$\zeta\frac{\partial u}{\partial\lambda}$	$\zeta\frac{\partial v}{\partial\phi}$	$\zeta\nabla\cdot\boldsymbol{u}$	$\frac{\partial}{\partial\lambda}(\omega\frac{\partial}{\partial p}v)$	$-\frac{\partial}{\partial\phi}(\omega\frac{\partial}{\partial p}u)$	F_{fr}	R
2.96e-03	2.56e-03	9.47e-05	3.34e-06	4.00e-05	4.85e-04	1.36e-05

List of Figures

1 Power spectrum density of the meridional geostrophic wind at 500 hPa and 50° N, from Fraedrich and Böttger (1978)((c)American Meteorological Society. Used with permission). 44

2 Scale map of the two asymptotic regimes considered: the single-scale planetary regime (PR) and the quasi-geostrophic (QG) regime. The two-scale PR model describes both regimes. See section 2a for an explanation of the units and of the small parameter ε. 45

3 Zonal wavenumber - frequency plot of the power spectral density for different terms in the model vorticity equation (48); all at 500 hPa and 50°N, all in units of Ω^4. In the title caption $f\frac{\partial u}{\partial \lambda}$ stands for $f\frac{1}{\cos\phi}\frac{\partial u}{\partial \lambda}$. 46

4 Same as in Fig. 3 but for a different wavenumber/frequency range. 47

5 Normalized standard deviation of $\nabla \cdot \boldsymbol{u}\zeta$ at 200 hPa (a,c) and at 500 hPa (b,d) as a function of the total wavenumber n. (a),(b) unfiltered data, (c),(d) low-pass filtered data (periods $\geq$ 10 d, see Blackmon (1976) for filter details). The standard deviation of a term V for some n is given by $\Sigma_n(V) = \sum_{k=1}^{n} \sigma_n^k(V)$, where $\sigma_n^k(V)$ denotes the standard deviation of the spectral coefficient of V for zonal wavenumber k and total wavenumber n. The normalization factor is $\frac{1}{4}(\Sigma_n(u\frac{\partial \zeta}{\partial \lambda}) + \Sigma_n(v\frac{\partial \zeta}{\partial \phi}) + \Sigma_n(\zeta\frac{\partial u}{\partial \lambda}) + \Sigma_n(\zeta\frac{\partial v}{\partial \phi}))$. 48

6 Normalized standard deviation of $f\nabla \cdot \boldsymbol{u}$ and $\nabla \cdot f\boldsymbol{u}$ at 200 hPa (a,c) and at 500 hPa (b,d) as a function of the total wavenumber n. The normalization factor is $\frac{1}{2}(\Sigma_n(f\frac{\partial u}{\partial \lambda}) + \Sigma_n(f\frac{\partial v}{\partial \phi}))$ and $\frac{1}{3}(\Sigma_n(f\frac{\partial u}{\partial \lambda}) + \Sigma_n(f\frac{\partial v}{\partial \phi}) + \Sigma_n(\beta v))$ for $f\nabla \cdot \boldsymbol{u}$ and $\nabla \cdot f\boldsymbol{u}$, respectively. (a),(b) unfiltered data, (c),(d) low-pass filtered data. See the description below Fig. 5 for explanation of the normalization factors. 49

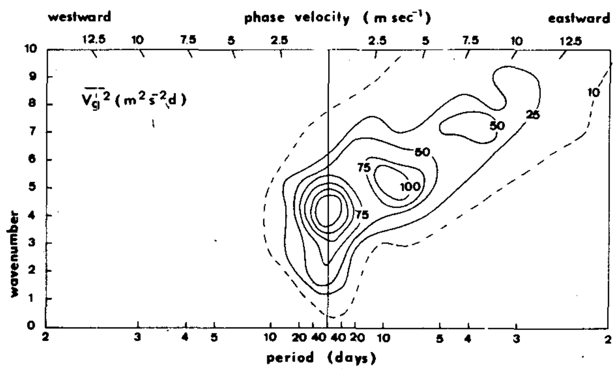

FIG. 1. Power spectrum density of the meridional geostrophic wind at 500 hPa and 50° N, from Fraedrich and Böttger (1978)((c)American Meteorological Society. Used with permission).

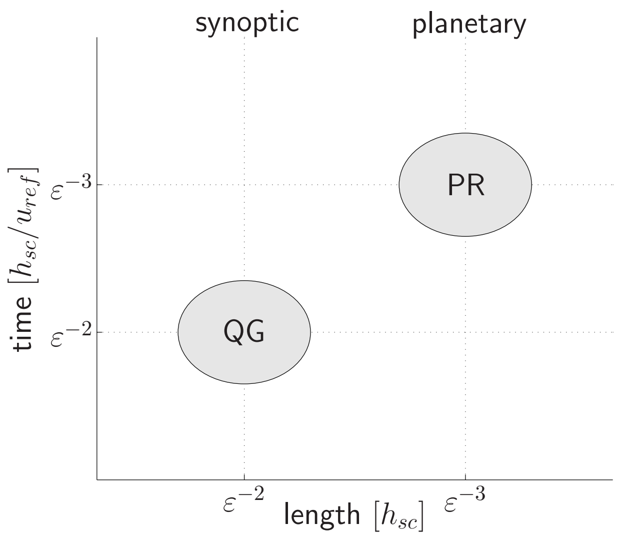

FIG. 2. Scale map of the two asymptotic regimes considered: the single-scale planetary regime (PR) and the quasi-geostrophic (QG) regime. The two-scale PR model describes both regimes. See section 2a for an explanation of the units and of the small parameter ε.

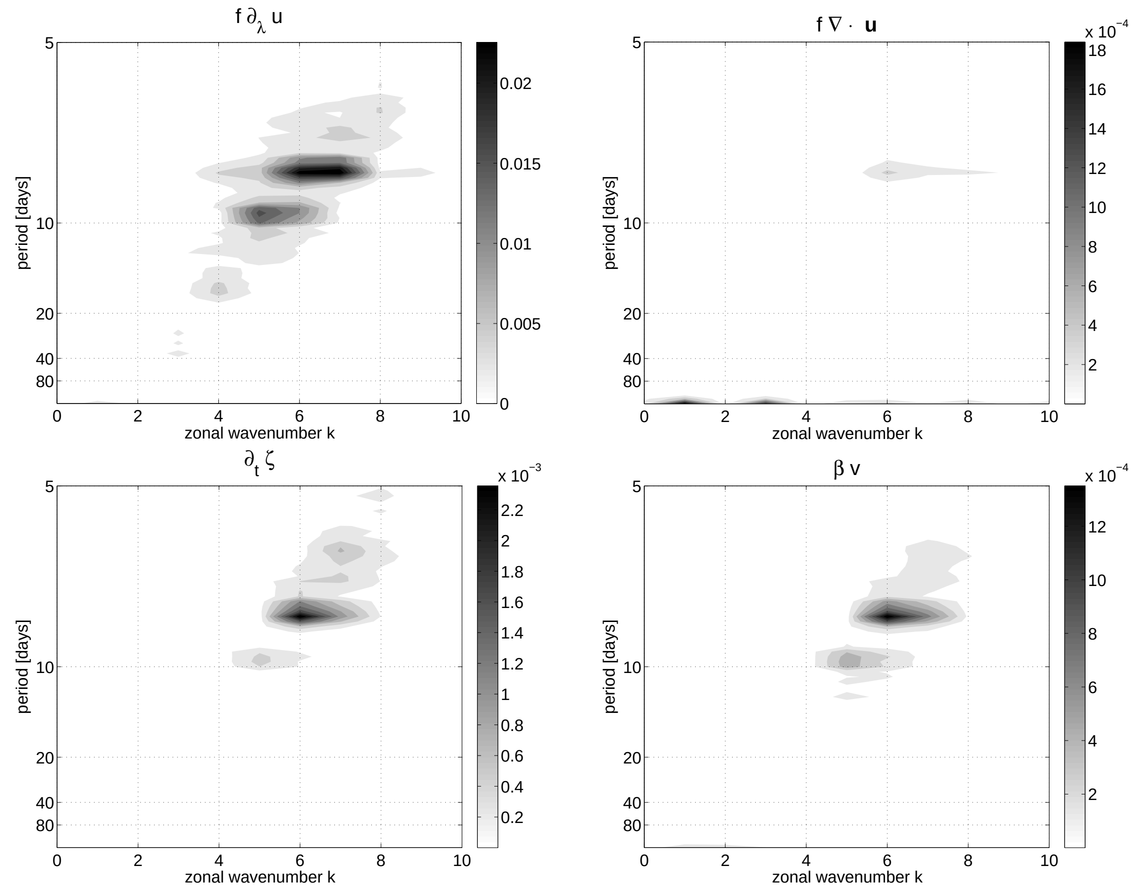

FIG. 3. Zonal wavenumber - frequency plot of the power spectral density for different terms in the model vorticity equation (48); all at 500 hPa and 50°N, all in units of Ω^4. In the title caption $f\frac{\partial u}{\partial \lambda}$ stands for $f\frac{1}{\cos\phi}\frac{\partial u}{\partial \lambda}$.

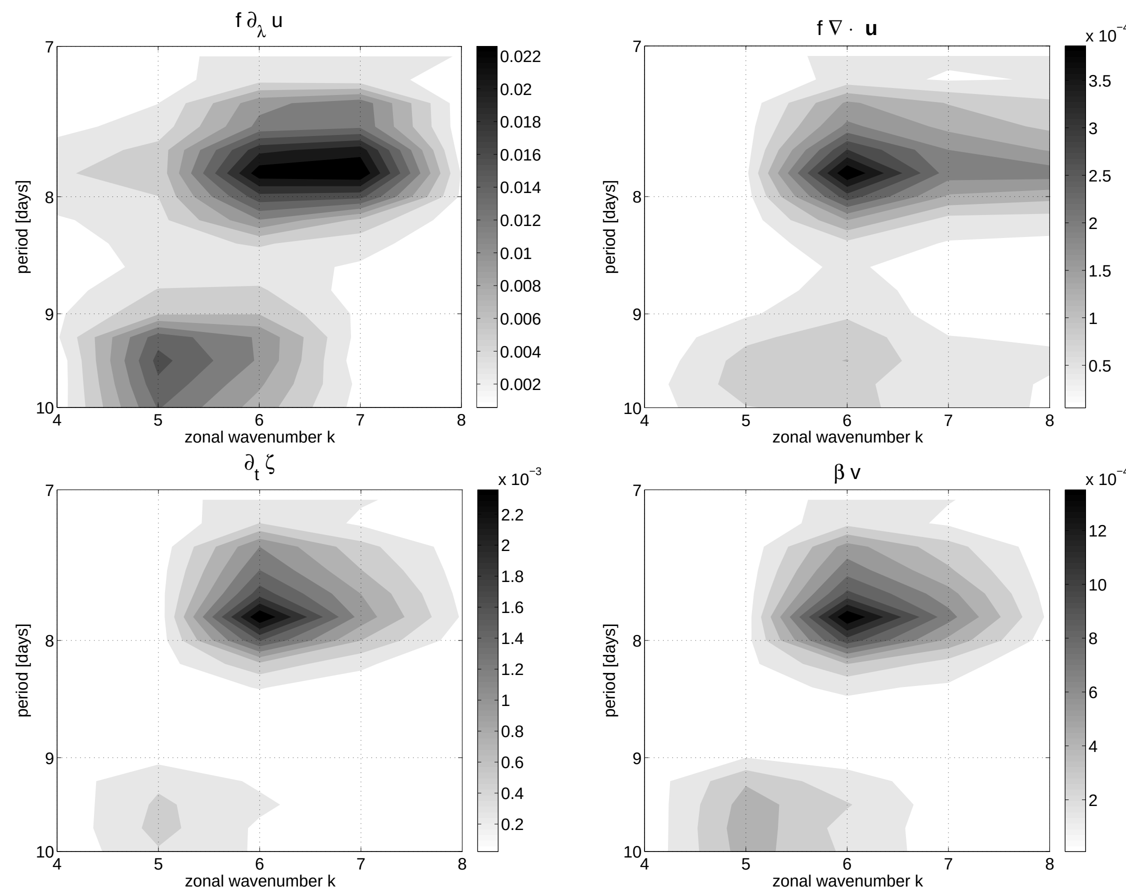

FIG. 4. Same as in Fig. 3 but for a different wavenumber/frequency range.

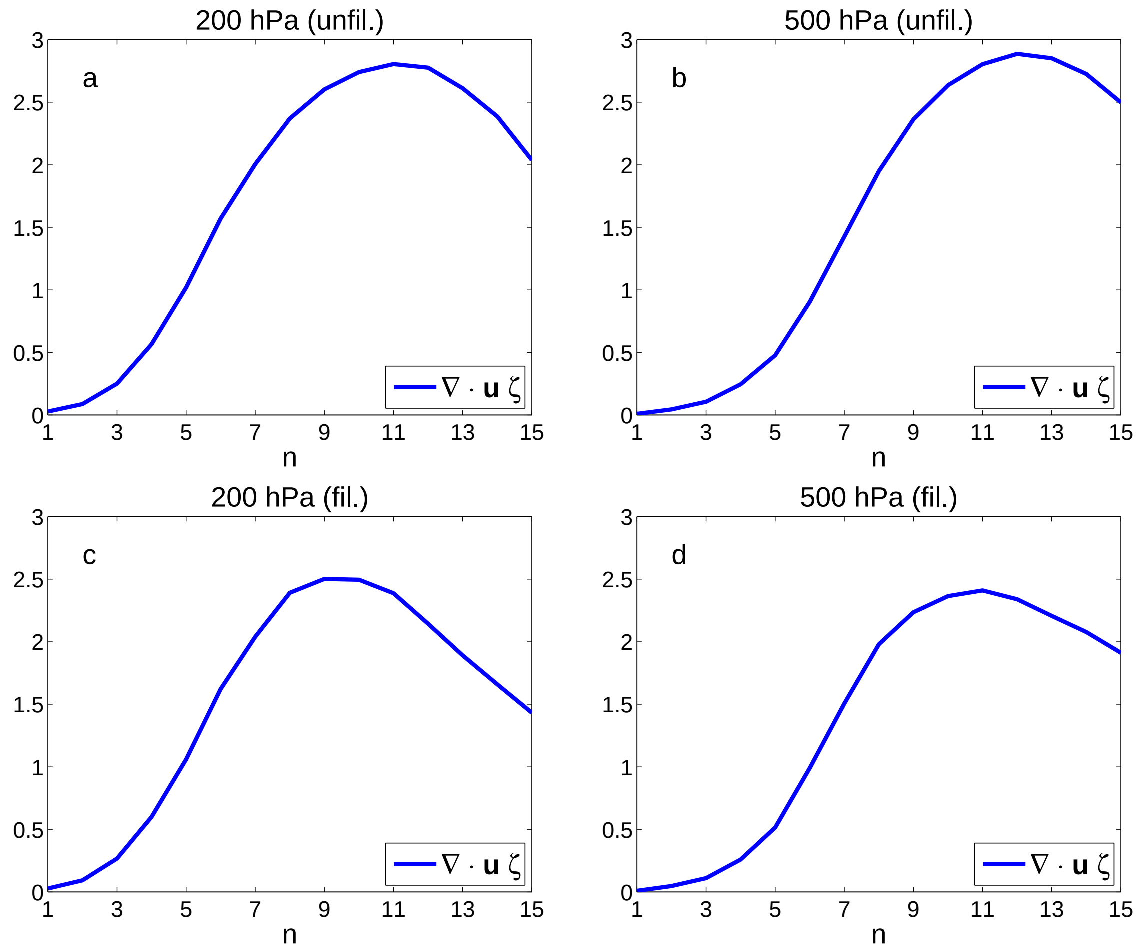

FIG. 5. Normalized standard deviation of $\nabla \cdot \boldsymbol{u}\zeta$ at 200 hPa (a,c) and at 500 hPa (b,d) as a function of the total wavenumber n. (a),(b) unfiltered data, (c),(d) low-pass filtered data (periods $\geq$ 10 d, see Blackmon (1976) for filter details). The standard deviation of a term V for some n is given by $\Sigma_n(V) = \sum_{k=1}^{n} \sigma_n^k(V)$, where $\sigma_n^k(V)$ denotes the standard deviation of the spectral coefficient of V for zonal wavenumber k and total wavenumber n. The normalization factor is $\frac{1}{4}(\Sigma_n(u\frac{\partial\zeta}{\partial\lambda}) + \Sigma_n(v\frac{\partial\zeta}{\partial\phi}) + \Sigma_n(\zeta\frac{\partial u}{\partial\lambda}) + \Sigma_n(\zeta\frac{\partial v}{\partial\phi}))$.

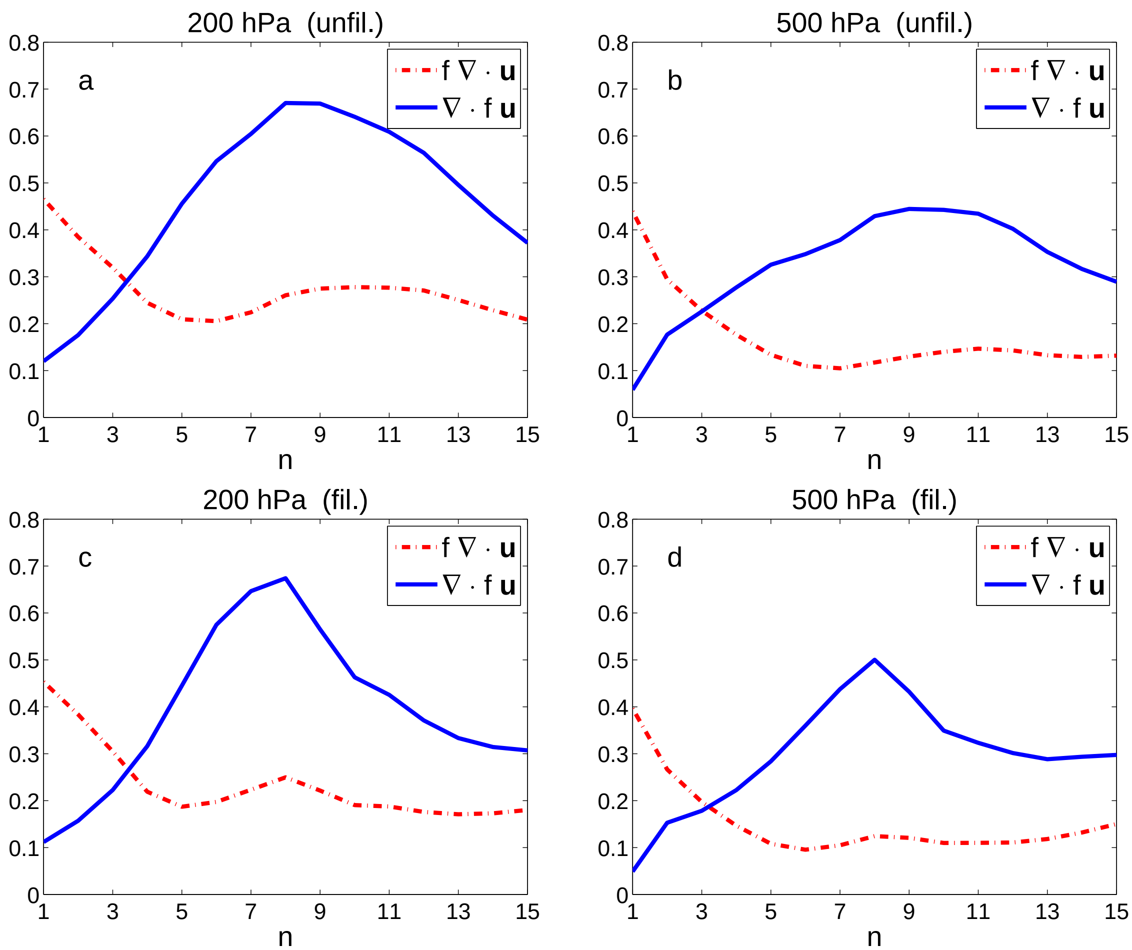

FIG. 6. Normalized standard deviation of $f\nabla \cdot \boldsymbol{u}$ and $\nabla \cdot f\boldsymbol{u}$ at 200 hPa (a,c) and at 500 hPa (b,d) as a function of the total wavenumber n. The normalization factor is $\frac{1}{2}(\Sigma_n(f\frac{\partial u}{\partial \lambda})+\Sigma_n(f\frac{\partial v}{\partial \phi}))$ and $\frac{1}{3}(\Sigma_n(f\frac{\partial u}{\partial \lambda})+\Sigma_n(f\frac{\partial v}{\partial \phi})+\Sigma_n(\beta v))$ for $f\nabla \cdot \boldsymbol{u}$ and $\nabla \cdot f\boldsymbol{u}$, respectively. (a),(b) unfiltered data, (c),(d) low-pass filtered data. See the description below Fig. 5 for explanation of the normalization factors.